

## Response to Editor

Comments to the Author:

Dear authors,

three reviewers have given feedback on your manuscript. The reviewers give generally very positive feedbacks and state they were intrigued by the analysis and results. All find that it is a timely and valuable contribution to the field of global hydrology. The paper is well structured and written. The reviewers have also given constructive feedback and criticism and you have addressed several of those comments in your response.

I agree with the assessment of the reviewers on the merit and novelty of the presented analysis. I would however like to emphasize one point: All of the reviewers comment, in one way or the other, on the fact that the results hinge upon the correctness of the CDR dataset. In your response you emphasize how carefully the CDR dataset was developed and validated, and also your own efforts to validate e.g. the standard deviation of  $E$ . I appreciate this. However, some of the standard variations in the dataset are not yet validated. I agree with reviewer #2 (René Orth) that a cross-validation would be desirable to learn whether the observed variance patterns are a property of the CDR dataset or hold with other datasets. At the very least, and since the main message of the manuscript is a call for investigation into the causes of the observed hydroclimatic variability, the discussion should more than now acknowledge to that fact that any efforts towards validation of those patterns are equally warranted.

Please submit the revised manuscript, with changes highlighted, together with a point by point response to all of the reviewers comments.

I thank both the authors and reviewers for the constructive discussion and look forward to the revised manuscript,

Anke Hildebrandt.

Response: We thank the editor for the evaluation and comment on the manuscript. As suggested by the editor and reviewers, we have carefully read and revised the manuscript accordingly as well as conducted a point-by-point response to all the comments.

The main comment here is a further cross-validation of the CDR data results based on atmospheric reanalysis (e.g., the state-of-the-art ERA5 dataset). As suggested by both editor and R2, in this response we report a comparison of the CDR ( $P$ ,  $E$ ,  $Q$  and  $\Delta S$ ) with the same from the recently released ERA5. We found  $P$  to be similar in both CDR and ERA5, but we found  $E$  and  $Q$  to be generally **much** higher in ERA5 compared to CDR (please see details in response to R2C3). As a consequence, in ERA5 we found that the sum of  $E$  and  $Q$  regularly exceeded  $P$  by large amounts. For example, in the Amazon,  $E$  and  $Q$  exceeded  $P$  by up to 1000 mm each and every year. So over a 27 year period, the predicted decline in storage in the Amazon region embedded in ERA5 approached 27000 mm (27 m)! This represents a major problem in the mass balance (or a lack of mass balance) in the ERA5 reanalysis and is physically not plausible. In contrast, over ice covered regions (e.g., Greenland), the hydrologic balance implied a continuing gain in storage of roughly similar magnitudes (i.e., 27 m in 27 years). Again, this is also physically not plausible.

Though the ERA5 is the state-of-the-art atmospheric reanalysis, we concluded that there was a major problem with the hydrologic (mass) balance and that the “atmospheric-centric” ERA5 database was not yet suitable for use in hydrologic studies.

As suggested by the editor, we also added the statement about the importance towards further improvement and validation of the patterns obtained in this manuscript in the revised manuscript.

Another important point raised by the reviewers (R2, R3) were (divergent) criticisms of the summary sections of the original manuscript. After carefully looking at comments from R2 and R3 and the structure and content of the original manuscript, we concluded that the underlying problem was that the original Discussion and Conclusions were repetitive and generally not well formulated. In response, we decided to combine the original sections (sections 5 and 6) into a new single section 5 (Discussion and Conclusions), and have streamlined the text accordingly by integrating the comments by reviewers. We believe that this has made the summary section more concise and that this change has substantially improved the manuscript.

We sincerely appreciate both the editor and reviewers for constructive suggestions and comments on the manuscript.

### **Response to Referee #1 (Anonymous)**

**In the following we use R1C1 (etc) to refer to comment 1 (C1) by referee 1 (R1).**

R1C1: This is an excellent paper with major implications to our understanding of long term water balance and their climatic and landscape controls.

Response: We thank the anonymous reviewer for the evaluation and positive comment on the manuscript.

R1C2: This kind of work could not have been even just a few years ago, but as more and more reanalysis data become available the ability to do this kind of work and learn from it improves (given the caveat that this is ultimately model generated data, but the best we have).

I have no problems with the analyses that have been done, and the presentation. The authors use monthly data but the analysis is about inter-annual variability, although they do use the monthly data to estimate the storage capacity. I would like to see a categorical statement about this, I found it confusing. This means they only have 28 years of data (28 numbers) - they need to make an assessment/statement about the implications of this for their estimates of the various statistics, given potential non-stationarities etc.

Response: In this initial investigation, we use the CDR (monthly database) and as the reviewer has noted this is an entirely new field of research since global hydrologic reanalysis data has not previously been available. We chose to focus on the inter-annual variability to establish links directly with important earlier work on this topic (e.g., Koster & Suarez, 1999). We plan to extend this work to a seasonal time scale in future research. To eliminate the potential confusion, we made a statement as the reviewer suggested in the revised version of manuscript:

(Lines 100-101): *“In this study we focus on the inter-annual variability and the monthly water cycle variables ( $P$ ,  $E$ ,  $Q$  and  $\Delta S$ ) are aggregated to annual totals.”*. Also, another statement about the limitations of 27-year study period has been added in the revision (Lines 457-460): *“The CDR is one of the first dedicated hydrologic reanalysis databases and includes data for a 27-year period. Accordingly, we could only examine hydrologic variability over this relatively short period. Further, we expect future improvements and modifications as the hydrologic community seeks to further develop and refine these new reanalysis databases.”*.  
Thanks.

R1C3: The main issue that I have with the paper is that (as the authors themselves admit) is the preliminary nature of the discussion and conclusions. The results, to say the least, are quite interesting and intriguing. Without further analysis, one can only speculate. The dependence on storage capacity and temperature are potential clues. This is a concern for me - one solution is to delay the paper until further analysis is done to elucidate these results. It seems the main route to explanations is to use the monthly data that they already have, to see if there is an extension of the variances and especially cross-covariances into the seasonal regime. In other words, I am speculating if the causes of the inter-annual variability lie in the intra-annual variability of the fluxes and the storage, and in the role of vegetation (and soils) buffering the variability in the climate.

Response: We agree with R1 about the likely importance of the seasonal (i.e. intra-annual) cycle to further explain these results. However, given the new approach developed in this manuscript we deliberately chose to publish the somewhat simpler inter-annual results first.

Please also see R1C2.

R1C4: For now there is a decision to be made - I am comfortable with going ahead with publication of the current paper (in spite of its preliminary nature) in view of the fact publication of the paper may trigger follow-on research by other research groups as well.

Response: We appreciate the comments of the reviewer.

## **Response to Referee #2 (Dr René Orth)**

R2C1: Review of Dongqin and Roderick “Inter-annual variability of the global terrestrial cycle”  
This study investigates the propagation of precipitation variability into the water cycle, i.e. into variations of runoff, evapotranspiration, and of storage changes. The authors show that this is mostly controlled by temperature (in wet regions), long-term aridity (in transitional regions), and by soil water storage capacity (in dry regions). Further, the results illustrate that the corresponding partitioning is different from the partitioning of mean precipitation into the means of these water cycle variables.

---

Recommendation: I think the paper requires major revisions.

The analysis is very interesting and provides new and fundamental insights into large-scale land surface hydrology. Related variability analyses are still not commonly done due to a lack of reliable data and underlying theory. This study can foster theory development in this area, and it underlines the importance of continuous improvement of the just-emerging global hydrological re-analysis datasets. Therefore I would be happy to see it published in HESS, but after some general revisions.

Response: We thank R2 for the evaluation and helpful comments on the manuscript.

R2C2: (1) Next to the consideration of the soil water storage capacity and the mean temperature to explain variations in the partitioning of precipitation variability, I am missing the inclusion of vegetation type as an explanatory variable. It might have strong implications on evapotranspiration variability, and therefore also on runoff and storage variabilities.

Response: We agree with Dr René Orth that the inter-annual variability might be related to the other factors, e.g., vegetation type. However, given the fact that this is a new approach and the research is exploratory, we focused on relating the inter-annual variability with the most general hydrologic factors (i.e., the air temperature as a surrogate for snow/ice and water storage capacity). We expect to extend the current work to a more complete analysis (e.g., relation to vegetation) in future research and we hope others will follow by examining factors like vegetation since this will require the effort of many scientists.

R2C3: (2) I agree with the authors that comprehensive hydrological reanalysis datasets are lacking, and the CDR dataset is an important contribution in that respect. Further, I appreciate the effort they make to validate the applicability of the dataset in the context of this study. However, also the CDR dataset is (necessarily) based on a model and hence it is not clear that the reported relationships are operating in nature, and not only in this model. To address this issue, I would like to see the key analyses from this study repeated with the state-of-the-art ERA5 reanalysis, which should be superior to ERA-Interim also in terms of land surface representation.

Response: As suggested by both R2 and the editor, we have compared the CDR ( $P$ ,  $E$ ,  $Q$  and  $\Delta S$ ) with the same from the recently released ERA5. For this comparison, we use the same 1984-2010 period. We downloaded monthly  $P$ ,  $E$  and  $Q$  (denoted as total runoff and calculated by ERA5 as surface plus sub-surface runoff) from the ERA5 website. The water storage change ( $\Delta S$ ) is not included in the ERA5 database, and we calculated it using mass balance for each individual month during 1984-2010. We then conducted further analysis and found  $P$  to be similar in both CDR and ERA5 (Fig. R1). However, we found  $E$  and (especially)  $Q$  to be generally **much** higher in ERA5 compared to CDR (Figs. R2-R3). This has important consequences for the change in storage as described below.

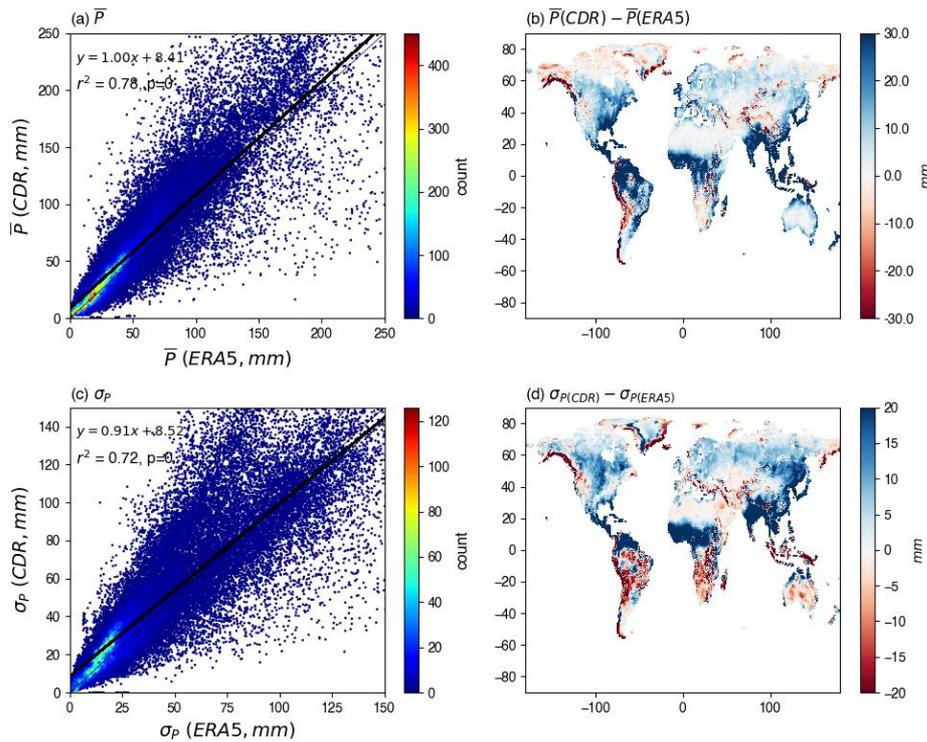


Figure R1. Comparison of monthly precipitation  $P$  between ERA5 and CDR databases. Top panels (a) (b) show comparison of the mean monthly ( $\bar{P}$ ) while bottom panels (c) (d) show comparison of the standard deviation ( $\sigma_P$ ) of monthly  $P$ .

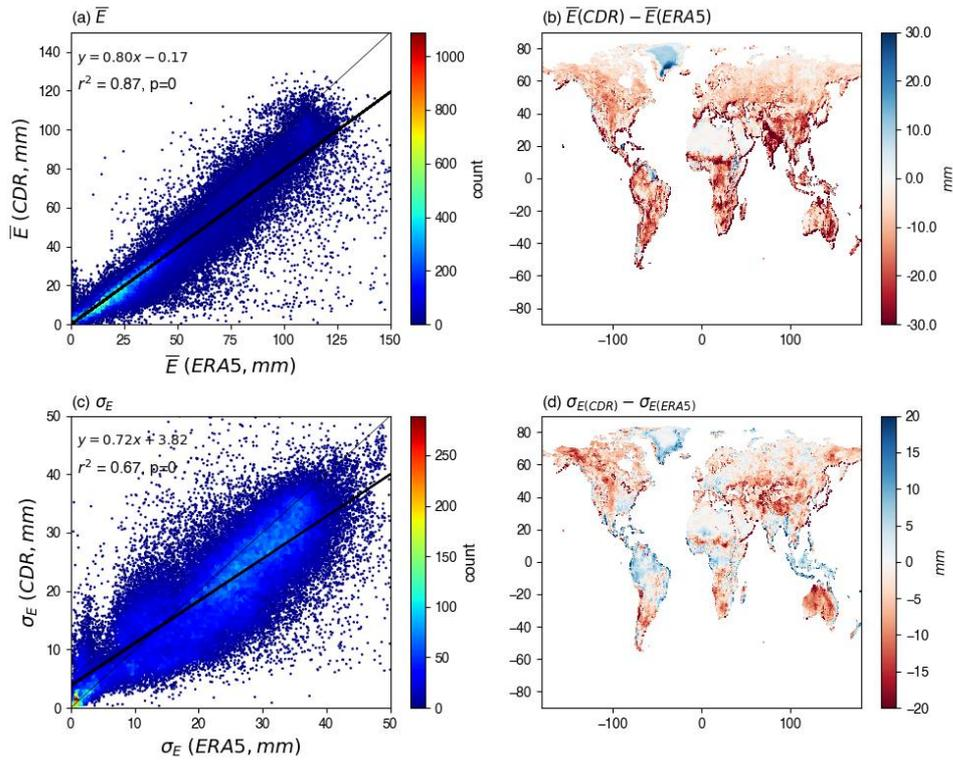


Figure R2. The same as Fig. R1 but using monthly evapotranspiration  $E$  from ERA5 and CDR databases.

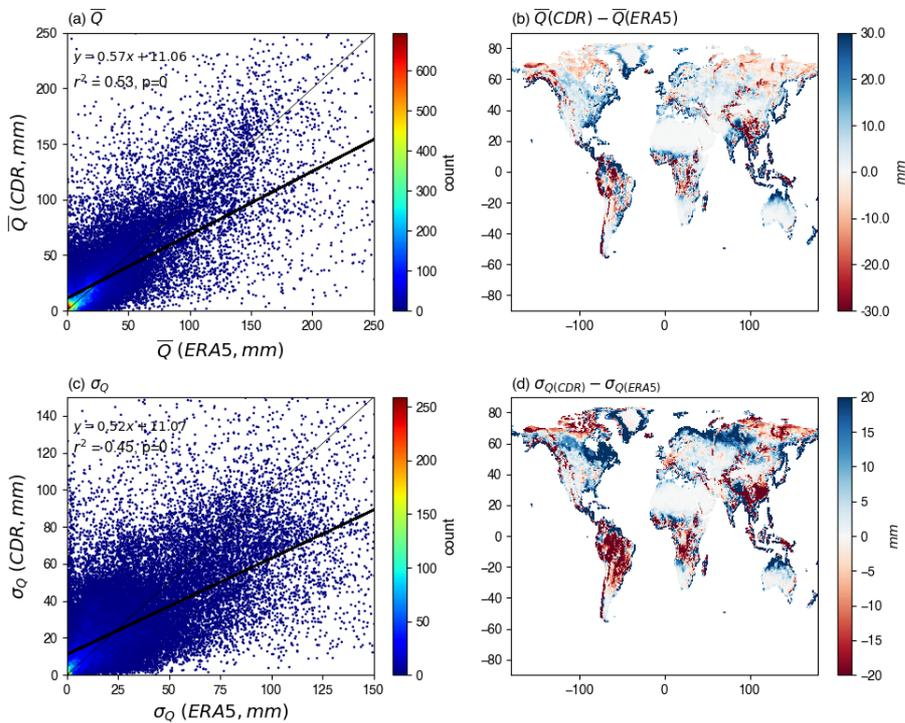


Figure R3. The same as Fig. R1 but using monthly runoff  $Q$  from ERA5 and CDR databases.

While the comparison with  $P$  (CDR vs ERA5 is reasonable, i.e., slope of the regression in Fig. R1a = 1.0), we find that  $E$  from ERA5 is on average 25% larger (i.e. slope is 0.8, see Fig. R2a) than  $E$  in CDR. Further,  $Q$  from ERA5 is on average 75% larger (i.e., slope is 0.57, see Fig. R3a) than  $Q$  in CDR. Now we know that in CDR, the mass balance was enforced. The obvious implication from these regressions is that in ERA5 the sum of  $E$  and  $Q$  must substantially exceed  $P$ .

To further evaluate ERA5, we then integrated the monthly data to annual totals. Visually, the results visually show similar global spatial patterns of long-term mean  $P$ ,  $E$  and  $Q$  in the ERA5 database (see the Fig. R4a-c) to those in the CDR database (see Fig. 1 in the revised manuscript). However, as noted above, the long-term mean annual water storage change ( $\Delta S$ , Fig. R4d) implied by ERA5 showed evidence of a major problem with the local hydrology. In particular, most regions of the earth surface show very large negative values for  $\Delta S$ , e.g., in the Amazon long term mean annual  $\Delta S$  is around -1000 mm. The implication is that over the 27-year period (1984-2010), the annual storage change in ERA5 over the Amazon region is -1000 mm every year and this equal 27 meters of storage change over the full period. This occurs in ERA5 because the sum of long-term mean annual  $E$  and  $Q$  is substantially greater than  $P$  in the Amazon. This is physically not plausible. The same problem holds for many other warm regions. In contrast, over the ice covered regions (e.g., Greenland), the hydrologic balance implied a continuing gain in storage. Again, this is physically not plausible.

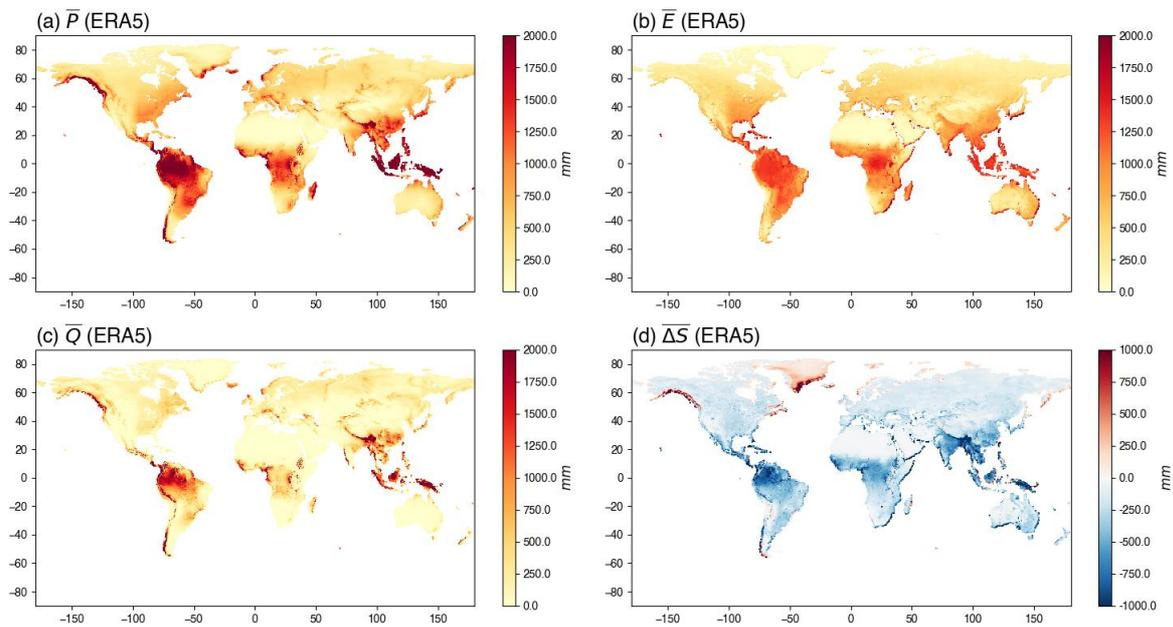


Figure R4. Mean annual (1984-2010) (a)  $P$ , (b)  $E$ , (c)  $Q$  and (d)  $\Delta S$  in the ERA5 database.

Though the ERA5 is the state-of-the-art atmospheric reanalysis, we concluded that there was a major problem with the hydrologic (mass) balance and that the “atmospheric-centric” ERA5 database was not yet suitable for use in hydrologic studies.

Returning to the suitability of the CDR database and its relation to the real world, there is ample evidence that it is suitable for the analysis conducted here including:

- (i) The enforcement of basic hydrologic concepts (mass balance).
- (ii) The numerous tests of CDR reported in the original Zhang et al 2018 HESS publication (that are summarized on lines 134-139 of the HESSD manuscript). Those tests include a (successful) comparison of CDR runoff to observations of monthly runoff at 165 medium size basins and 862 small basins. In fact, the assessment of CDR in the original paper was quite comprehensive as you would expect.
- (iii) We have augmented those extensive original tests by independently comparing monthly  $E$  with FLUXNET tower data at 32 sites which confirmed that the CDR captured the general seasonal cycle in both  $P$  and  $E$  at those 32 sites (Fig. S3, S4, S5, Table S1 in the revised manuscript). We also used the same FLUXNET data to compare the variability in  $P$  with variability in  $E$  (Fig. S6 in the revised manuscript).
- (iv) We further compared CDR  $E$  with two gridded  $E$  databases that are not included in the source databases of CDR (LandFluxEval, MPI, see lines 159-166 in the revised manuscript and Fig. S7, S8) and the comparison was satisfactory.
- (v) We compared how the standard deviation for  $E$  and the mean for  $E$  are related in the CDR (Fig. 4 in the revised manuscript) and compared that with the same relations in LandFluxEval and MPI (Fig. S10 in the revised manuscript). Those two comparisons were satisfactory.
- (vi) The mean water cycle ( $P$ ,  $E$ ,  $Q$ ) in CDR was shown to be consistent with the long-standing Budyko framework (Fig. 2 in the revised manuscript).
- (vii) The CDR data were consistent with the Koster & Suarez (1999) theory in the limit of sites that have limited water storage (Fig. 5 in the revised manuscript).

That is a very comprehensive assessment.

Further, we readily acknowledge that the CDR database is the first hydrologic reanalysis and we expect more ‘hydrologic-centered’ databases to compare it to in the near future. For that reason we chose to only investigate the most general factors that we believe will stand the test of time and we have also described the study as an initial exploratory survey at several places in the manuscript.

R2C4: (3) I appreciate the idea of investigating the influence of the soil water storage capacity and the mean temperature on the variability partitioning. However, I think parts of the conclusions drawn by the authors from Figures 8-10 are not supported by the data. For example, I cannot see in Figure 10 that the temperature influence is particularly strong in very wet regions. Rather, to me it seems to be strong in moderately wet and dry regions (Fig 10b,d,f,h,j,l,n,p). Further, also the aridity limit of 6 which the authors suggest in their interpretation of the results in Figure 9, is arbitrary and not supported by the actual results. Storage capacity is obviously having an influence already for aridity values above 2-3 (Fig. 9b,c,f,j,k). Overall, in these Figures there are many interesting patterns but the authors focus only on few sub-plots and limit their interpretation to these. Therefore, I suggest to either show less information/sub-plots there, or to develop explanations also for patterns emerging within other sub-plots.

Response: We accept that Fig. 10 (Fig. 8 in the revised manuscript) is hard to interpret. On reading the reviewers comments and going over the manuscript we realize the problem was that we did not explicitly indicate the relevant panels (i.e., a, b, c, ....) and the text was not well-formulated. This was an oversight correctly identified by the reviewer. In general, the data in Fig. 10 was not particularly revealing (i.e., a negative result) but we actually focused the discussion to the first and third columns but we did not identify them properly. In response, we replaced the original text with the following (lines 307-314):

*“To understand the potential role of snow/ice in modifying the variance partitioning, we repeat the previous analysis (Fig. 7) but here we use the mean annual air temperature ( $\overline{T}_a$ ) to colour the grid-cells to (crudely) indicate the presence of snow/ice (Fig. 8). The results are complex and not easy to simply understand. The most important difference revealed by this analysis is in the hydrologic partitioning between cold (first column) and hot (third column) conditions in wet environments ( $\overline{E}_o/\overline{P} \leq 0.5$ ). In particular, when  $\overline{T}_a$  is high,  $\sigma_p^2$  is almost completely partitioned into  $\sigma_Q^2$  in wet environments (e.g.,  $\overline{E}_o/\overline{P} \leq 0.5$ , Fig. 8g). In contrast, when  $\overline{T}_a$  is low in a wet environment ( $\overline{E}_o/\overline{P} \leq 0.5$  in first column of Fig. 8), there are substantial variations in the hydrologic partitioning. That result reinforces the complexity of variance partitioning in the presence of snow/ice.”*

R2C5: (4) The paper contains (too) many figures, which is diluting the main message(s), I feel. For example, Figures 1 and 2 could be merged, Figure 5 could be moved to the supplementary material, Figure 13 could be merged into Figure 8. The authors might have further ideas to reduce the amount of figures. Moreover, I do not really understand the difference between Figures 7 and 8, and why both are needed.

I do not wish to remain anonymous - René Orth.

Response: We respect the reviewer’s opinion that we have too many figures – this is always a hard balance to get right to everyone’s satisfaction. We have moved the original Fig. 1 and Fig. 5 to the supporting material as suggested. There are now 12 figures in the revised manuscript with another 12 in the supporting material. However, we do not think the original Fig. 13 (Fig. 11 in the revision) should be merged into original Fig. 8 (Fig. 6 in the revision) since the two figures belong to different sections (original Fig. 8 for the relation between variance partitioning and aridity section, original Fig. 13 for the case study section). Original Fig. 7 (Fig.5 in the revision) is a direct link to previous work while original Fig. 8 is the variance partitioning in the CDR database. Hence while these two figures are similar, they make separate independent contributions to the manuscript.

---

Specific comments:

R2C6: line 8: Equation 2 not introduced yet line 13: It should be ‘variabilities’.

Response: We have deleted the text ‘Eq. 2’ and changed ‘the variability...’ to ‘that variability...’ to make the text clear to understand in the revised version of manuscript. Thanks.

R2C7: line 15: Some word is missing towards the end of the line

Response: We have checked line 15 in the original manuscript and did not find missing words?

R2C8: lines 35-39: Orth & Destouni (2018) might be relevant in this context and could be cited.

Response: The reference has now been cited in the revised manuscript.

R2C9: line 37: Not sure I get the point here.

Response: We mean that droughts and floods are typical extremes but that hydrologic variability encompasses more than just droughts and floods, i.e., hydrologic variability occurs across all time-space scales.

R2C10: lines 106-118: Please clarify that what you are determining here is actually not the soil water storage capacity, but rather the active range within which the soil moisture varies.

Response: Yes, exactly. We have modified the text and state the calculation to make this explicit in Lines 108-110 in the revised manuscript: “*For the storage, the active range of the monthly water storage variation was used to approximate the water storage capacity ( $S_{max}$ ).*”.

R2C11: lines 157-163: I would recommend to replace the LandFluxEVAL and the Jung et al. datasets with more recent gridded ET datasets such as the Jung et al. 2019 dataset and the GLEAM dataset (Martens et al. 2017).

Response: The reason we chose the LandFluxEVAL and MPI databases is that they are among the most widely used and validated  $E$  data that were also **not used** to develop the CDR database. We do not think adding a comparison to the latest GLEAM database would be as useful since an earlier version of GLEAM (v2a) was actually an input to the data assimilation scheme used to construct the CDR (see Table 1 in Zhang et al., 2018, HESS). Instead, the more appropriate approach would be to revise the CDR data assimilation but incorporating the latest GLEAM database but that is well beyond the scope of this work. (Also see R2C3 for similar comments about ERA.) We could replace the MPI we used with the updated database (Jung et al., 2019) but we do not see how that would alter the results.

R2C12: line 180: Gudmundsson et al. (2016) might be relevant in this context and could be cited.

Response: The reference has been cited in the revised manuscript. Thanks.

R2C13: line 181: What is meant by seasonality here? I thought you are considering annual data? In general, I think the considered temporal and spatial scales and resolution need to be more clearly stated and motivated at the beginning of the manuscript. Also, the role of these decisions on the results could be discussed.

Response: Yes, we are using annual data. But we know that differences of the intra-year seasonal timing (phase) of precipitation and  $E_0$  do have an effect on the annual water balance (as per the seminal work by Chris Milly in the early 1990s.). To make this more clear, we have added a statement in the revised manuscript (Lines 100-101): “*In this study we focus on the inter-annual variability and the monthly water cycle variables ( $P$ ,  $E$ ,  $Q$  and  $\Delta S$ ) to annual totals.*”

Given the initial stage for this type of research and our plan to include the seasonal variations in future work (also see R1C2 and R1C3), a statement has been added in the revised manuscript (Lines 505-508): “*That result demonstrates that deeper understanding of the process-level interactions that are embedded within each of the three covariance terms (e.g., the role of seasonal vegetation variation) will be needed to develop process-based understanding of variability in the water cycle in these biologically productive regions ( $0.5 < \overline{E}_o/\overline{P} < 1.5$ ).*”.

R2C14: line 252/253: I could not find this discussion in section 5!? Would be important to explain these discrepancies, though.

Response: Thanks for pointing this oversight out. The underlying scientific issue here is that the original Koster and Suarez (1999) work assumed negligible water storage change. In that sense the original results of Koster and Suarez (1999) can be seen as an upper limit and any variance in storage can only reduce the partitioning of variability in  $P$  to variability in  $E$  under dry conditions (Fig. 7). We have added a short discussion on this in the revised manuscript (Lines 488-492): “*This result explains the overestimation of  $\sigma_E/\sigma_P$  by the empirical theory of Koster and Suarez (1999) which implicitly assumed no inter-annual change in storage. The Koster and Suarez empirical theory is perhaps better described as an upper limit that is based on minimal storage capacity, and that any increase in storage capacity would promote the partitioning of  $\sigma_P^2$  to  $\sigma_{\Delta S}^2$  particularly under dry conditions (Figs. 10-12).*”.

R2C15: line 327 & 333: ‘leaving very limited variance’ - not really true given your statement in lines 385-387

Response:

324 We show the  $P$ ,  $E$ ,  $Q$  and  $\Delta S$  time series along with the relevant variances and covariances in Fig. 12. Starting  
325 with the two dry sites, at the site with low storage capacity (Site 1), the time series shows that  $E$  closely follows  
326  $P$  leaving annual  $Q$  and  $\Delta S$  close to zero (Fig. 12a). The variance of  $P$  ( $\sigma_P^2 = 206.9 \text{ mm}^2$ ) is small and almost  
327 completely partitioned into the variance of  $E$  ( $\sigma_E^2 = 196.9 \text{ mm}^2$ ), leaving very limited variance for  $Q$ ,  $\Delta S$  and all  
328 three covariance components (Fig. 12b). At the site with high storage capacity (Site 2),  $E$ ,  $Q$  and  $\Delta S$  do not simply  
329 follow  $P$  (Fig. 12c). As a consequence, the variance of  $P$  ( $\sigma_P^2 = 2798.0 \text{ mm}^2$ ) is shared between  $E$  ( $\sigma_E^2 = 1150.2$   
330  $\text{mm}^2$ ),  $\Delta S$  ( $\sigma_{\Delta S}^2 = 800.5 \text{ mm}^2$ ) and their covariance component ( $2\text{cov}(E, \Delta S) = 538.4 \text{ mm}^2$ , Fig. 12d). Switching  
331 now to the remaining wet and hot site (Site 3),  $Q$  closely follows  $P$ , with  $\Delta S$  close to zero and  $E$  showing little  
332 inter-annual variation (Fig. 12e). The variance of  $P$  ( $\sigma_P^2 = 57374.4 \text{ mm}^2$ ) is relatively large and almost completely  
333 partitioned into the variance of  $Q$  ( $\sigma_Q^2 = 57296.4 \text{ mm}^2$ ), leaving very limited variance for  $E$  and  $\Delta S$  and the three  
334 covariance components (Fig. 12f). We also examined numerous other sites with similar extreme conditions as the  
335 three case study sites and found the same basic patterns as reported above.

The text here refers to the site-based case studies (line 327 – Fig. 12a (Fig. 10 in the revised manuscript) – Site 1; line 333 – Fig. 12 f – Site 3) while the later text (lines 385-387) refers to the general pattern across all grid-boxes, i.e., Fig. 4 (Fig. 3 in the revised manuscript). We have corrected this misunderstanding by rewriting lines 385-387 (lines 470-478 in revised manuscript) to indicate the relevant figures as follows:

*“With that in mind, we were surprised that the inter-annual variability of water storage change ( $\sigma_{\Delta S}^2$ ) is typically larger than the inter-annual variability of evapotranspiration ( $\sigma_E^2$ ) (cf. Fig. 3b and 3d). The consequence is that  $\sigma_{\Delta S}^2$  is more important than  $\sigma_E^2$  for understanding inter-annual variability of global water cycle. A second important generalisation is that unlike the variance components which are all positive, the three covariance components in the theory (Eq. 2) can be both positive and negative. We report results here showing both large positive and negative values for the three covariance terms (Fig. 3efg). This was especially prevalent in biologically productive regions ( $0.5 < \overline{E_o}/\overline{P} < 1.5$ , Fig. 3eg).”*

R2C16: lines 403-405: I cannot see this from Figure 8.

Response: Agreed. That was our mistake. The reference to Fig. 8 (Fig. 6 in the revised manuscript) should be to Fig. 4 (Fig. 3 in the revised manuscript, global pattern of water cycle variability) and we have revised that in the revision.

R2C17: Section 5: Overall a bit lengthy with too much summarizing, I think. Could be shorter, and more concise.

Response: Both R2 & R3 (see R3C4) had divergent views about the summary sections of our original manuscript.

After looking at both comments (R2, R3) and the structure of the original manuscript, we concluded that the original Discussion and Conclusions sections were repetitive and not well formulated.

In response, we have combined the original sections into a single section 5 (Discussion and Conclusions) and have streamlined the text accordingly. We believe that this has substantially improved the manuscript.

R2C18: Figure 3: Why are there data points outside the physically plausible range?

Response: We assume you mean points with  $E$  exceeding  $P$ ? This is possible in for example, regions with run-on, or irrigation. We have further investigated those points and also find that some of them come from the parts of Greenland that had not been masked out (Fig. 1).

R2C19: Figure 4: Many values seem to be cut at 10 as this is the end of the color bar. You could use log scale here for the color bar.

Response: Yes, the scale for  $P$  in Fig. 4a (new Fig. 3a in the revised manuscript) is saturated with the maximum value of the color bar 10,000. The reason we chose 10,000 as the limit was to show the patterns for both the relatively high (e.g.,  $\sigma_P^2$ ,  $\sigma_Q^2$  and  $\sigma_{\Delta S}^2$ ) and low variabilities (e.g.,  $\sigma_E^2$ ,  $2\text{cov}(E, \Delta S)$ ) while keeping the same scale for all panels. We have tried to modify this figure by using a log scale (see Fig. R5) to mitigate saturation, but it made the spatial patterns very difficult to distinguish compared with Fig. 3 in the revised manuscript (original Fig. 4) especially for the covariance panels (Fig. R5e-g). Therefore, we thought it better to keep the original legend in Fig. 3.

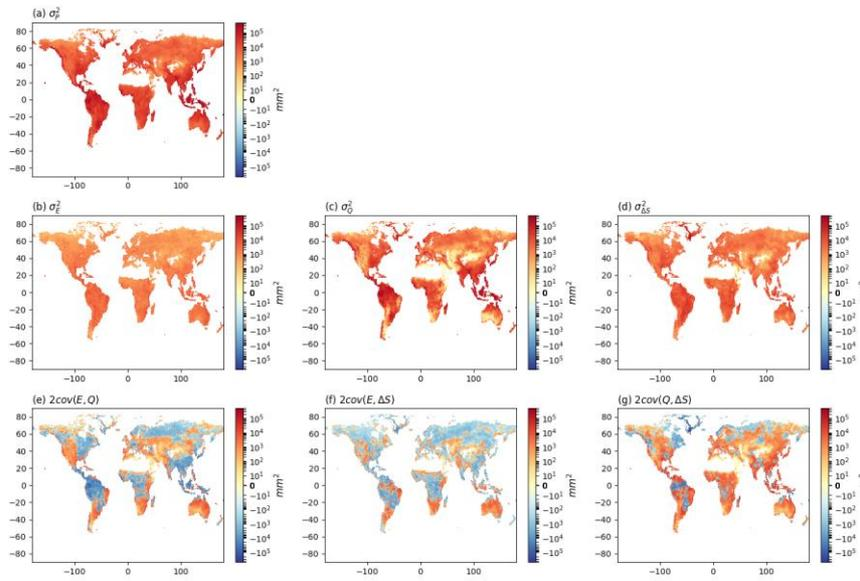


Figure R5. Water cycle variances ( $\sigma_P^2$ ,  $\sigma_E^2$ ,  $\sigma_Q^2$ ,  $\sigma_{\Delta S}^2$ ) and covariances ( $cov(E, Q)$ ,  $cov(E, \Delta S)$ ,  $cov(Q, \Delta S)$ ). Note that we have multiplied the covariances by two (see Eq. 2).

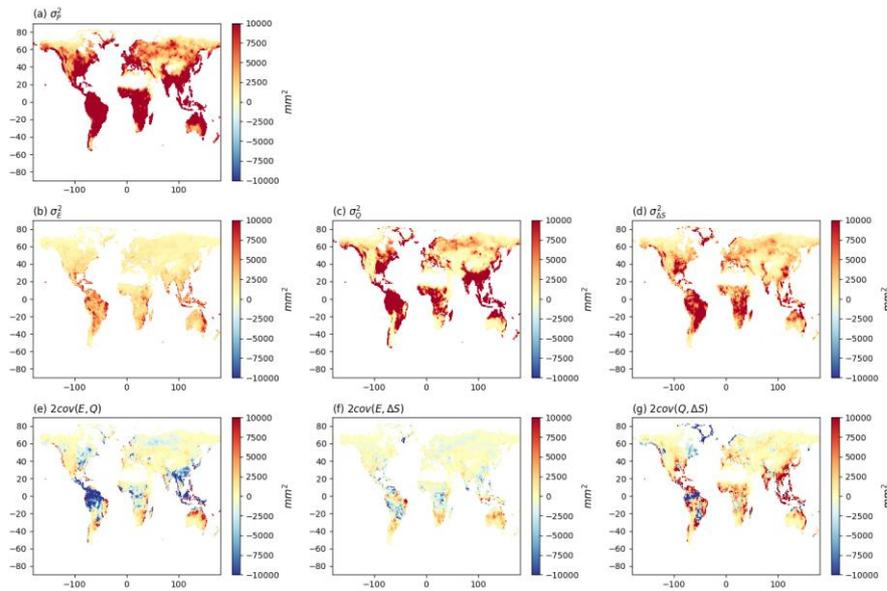


Figure 3 (original Figure 4). Water cycle variances ( $\sigma_P^2$ ,  $\sigma_E^2$ ,  $\sigma_Q^2$ ,  $\sigma_{\Delta S}^2$ ) and covariances ( $cov(E, Q)$ ,  $cov(E, \Delta S)$ ,  $cov(Q, \Delta S)$ ). Note that we have multiplied the variances by two (see Eq. 2).

R2C20: References:

Gudmundsson, L., P. Greve, and S. I. Seneviratne, 2016: The sensitivity of water availability to changes in the aridity index and other factors—A probabilistic analysis in the Budyko space, *Geophys. Res. Lett.* 43 (13), 6985-6994.

Jung, M., S. Koirala, U. Weber, K. Ichii, F. Gans, G. Camps-Valls, D. Papale, C. Schwalm, G. Tramontana, and M. Reichstein, 2019: The FLUXCOM ensemble of global land-atmosphere energy fluxes. *Scientific Data*, 6 (74).

Martens, B., D. G. Miralles, H. Lievens, R. van der Schalie, R. A. M. de Jeu, D. Fernández-Prieto, H. E. Beck, W. A. Dorigo, and N. E. C. Verhoest, 2017: GLEAM v3: satellite-based land evaporation and root-zone soil moisture, *Geosci. Model Dev.* 10, 1903–1925.

Orth, R., and G. Destouni, 2018: Drought reduces blue-water fluxes more strongly than green-water fluxes in Europe. *Nature Communications*, 9, 3602, doi: 10.1038/s41467-018-06013-7

Response: We appreciate Dr René Orth for listing all the reference mentioned above in the comments, and we have read and cite these reference accordingly in the revised manuscript. Thanks.

### Response to Referee #3 (Anonymous)

R3C1: This study tries to partition the inter-annual variability in precipitation ( $P$ ), i.e., the source term in terrestrial water cycle, into variabilities in three sink terms in terrestrial water cycle ( $ET$ ,  $Q$ ,  $\Delta S$ ), and then to relate the partitioning of variabilities to various factors like temperature, aridity, and storage capacity. I think this type of study at global scale is rather new, if not first of its kind at global scale, and thus very interesting to the hydrology community. This is the case mostly because there has been a lack of “hydrologic reanalysis” (CDR) for such kind of analysis in the first place. At the same time, this effort couldn’t fully answer many of the questions set forth at the beginning, leaving perhaps “more questions than answers” (as phrased by another referee). The authors have done a solid amount of thorough analysis and experiments toward the questions of interest and these analyses are also well designed too.

Overall I consider this manuscript of good quality, both scientifically and technically, and thus publishable in HESS with several concerns addressed.

Response: We agree that this is a first-of-its-kind study and thank the referee for the encouraging positive comments on the manuscript.

R3C2: My primary concern is there is a lack of general “signal-to-noise” discussions to better inform readers to what extent the findings are significant signals from the underlying data (CDR, Zhang et al., 2018) and how much of it could be due to data uncertainties (or possible artifacts due to how the data is produced). For example, the  $ET$  products that went into the CDR (satellite products, reanalysis, etc.) share some similarity in their production methods (e.g., Penman-Monteith or Priestley-Taylor type of schemes). Such similarity may limit the variability of  $ET$  in CDR. Of course, the plants do apply a strong filter on the inter-annual variability based on their survival need. Such uncertainty analysis may be difficult but I think some qualitative and general assessment would be very beneficial.

Response: The CDR uses a formal data assimilation scheme based on mass balance that weights the various inputs, and thereby produces uncertainty estimates for each variable ( $P$ ,  $E$ ,  $Q$ ,  $\Delta S$ ). The original paper (Zhang et al., 2018 HESS) includes a formal assessment of the sensitivity of  $P$ ,  $E$ ,  $Q$  over large regions (continents, basins) using the coefficient of variation (see original Figures 2, 3, 4, 5, 6, 7 in Zheng et al., 2018 HESS). We actually followed from that work and used those uncertainty estimates (lines 124-132 in the revised manuscript) to identify and mask out regions where the uncertainty was large relative to the magnitude of the fluxes. This screening procedure removed most grid-boxes from the Himalayas, Sahara Desert and Greenland (see Fig. S2 in the revised manuscript).

Secondly, while it is true that some of the products might share similarity in producing, for example,  $E$  (Penman-Monteith, Priestley-Taylor as the examples noted by the reviewer) the data assimilation is a comprehensive approach that includes all available estimates of  $P$ ,  $E$ ,  $Q$  and  $\Delta S$  at each grid box. With mass balance enforced, the CDR estimates represent a composite product that is designed to avoid bias of the type described by the reviewer as much as possible by using all available estimates of the hydrologic fluxes. As we have described in a response to Reviewer 2 (see R2C3), the CDR has been extensively validated in the original publication.

In that context, our goal was not to assess the CDR, but rather to use it for this “first-of-a-kind” study on the sources and sinks of inter-annual hydrologic variability. We have added words at the end of the manuscript that we expect further improvement and validation of obtained patterns (Lines 459-460): “*Further, we expect future improvements and modifications as the hydrologic community seeks to further develop and refine these new reanalysis databases.*”.

R3C3: Also, at the scale of the CDR (0.5 degree), I would say the partitioning is more complicated than just a result of several factors. The horizontal transport of water, seasonality, local water use, etc., can add a lot of noise. I wouldn't say it is not possible to do it at 0.5 degree, but it would probably be less noisy at a slightly coarser scale. Also, there could be much more controlling factors for the partitioning than being investigated, e.g., land cover/land use, LAI, topography.

Response: We agree with the reviewer that the partitioning is complex and could be related to the other factors, e.g., land cover/land use, LAI and horizontal transport of water due to topography, etc. In this first-of-a-kind analysis we chose to focus on the zero'th order physical factors (storage capacity, snow/ice) at the CDR data resolution (0.5 degree), but we fully expect more detailed analysis to follow, e.g., vegetation plant-based variables as discussed by the reviewer. We have added new text in the last paragraph of section 4.5 that speculates on the important role of vegetation processes that addresses this comment by R3. We have also emphasized that again in the final concluding paragraph of the manuscript.

R3C4: Finally, given that this study does tend to raise more questions than answers, I feel the authors should provide some more insights on what we can do from the analysis and findings in this study. What can we do with the numbers concluded here? Validating models? Improving single models like Budyko? Hydrologic/water risk analysis? Climate system behavior/sensitivity and hydrologic impacts of climate changes? And how can we improve our understanding in the future? What kind of new data at what scales would be critical to answering such questions? I feel this paper is incomplete without offering some of such insights.

Response: Please also see R2C17.

In further response, we have modified the final paragraph to set out a rough guideline for future research (lines 511-515): “*The hydrologic data needed to understand hydrologic variability are only now becoming available. With those data we can begin to develop a process-based understanding of hydrologic variability that can be used for a variety of purposes, e.g., deeper understanding of hydro-climatic behaviour, hydrologic risk analysis, climate change assessments and hydrologic sensitivity studies are just a few applications that spring to mind.*”.

# Inter-annual variability of the global terrestrial water cycle

Dongqin Yin<sup>1,2</sup>, Michael L. Roderick<sup>1,2,3</sup>

<sup>1</sup>Research School of Earth Sciences, Australian National University, Canberra, ACT, 2601, Australia

<sup>2</sup>Australian Research Council Centre of Excellence for Climate System Science, Canberra, ACT, 2601, Australia

<sup>3</sup>Australian Research Council Centre of Excellence for Climate Extremes, Canberra, ACT, 2601, Australia

Correspondence to: ([dongqin.yin@anu.edu.au](mailto:dongqin.yin@anu.edu.au))

## Abstract:

1 Variability of the terrestrial water cycle, i.e., precipitation ( $P$ ), evapotranspiration ( $E$ ), runoff ( $Q$ ) and water storage  
2 change ( $\Delta S$ ) is the key to understanding hydro-climate extremes. However, a comprehensive global assessment  
3 for the partitioning of variability in  $P$  between  $E$ ,  $Q$  and  $\Delta S$  is still not available. In this study, we use the recently  
4 released global monthly hydrologic reanalysis product known as the Climate Data Record (CDR) to conduct an  
5 initial investigation of the inter-annual variability of the global terrestrial water cycle. We first examine global  
6 patterns in partitioning the long-term mean  $\bar{P}$  between the various sinks  $\bar{E}$ ,  $\bar{Q}$  and  $\bar{\Delta S}$  and confirm the well-known  
7 patterns with  $\bar{P}$  partitioned between  $\bar{E}$  and  $\bar{Q}$  according to the aridity index. In a new analysis based on the concept  
8 of variability source and sinks (Eq. 2) we then examine how variability in the precipitation  $\sigma_P^2$  (the source) is  
9 partitioned between the three variability sinks  $\sigma_E^2$ ,  $\sigma_Q^2$  and  $\sigma_{\Delta S}^2$  along with the three relevant covariance terms, and  
10 how that partitioning varies with the aridity index. We find that the partitioning of inter-annual variability does  
11 not simply follow the mean state partitioning. ~~Instead we find that, with  $\sigma_P^2$  is~~ mostly partitioned between  $\sigma_Q^2$ ,  $\sigma_{\Delta S}^2$   
12 and the associated covariances. We also find that the magnitude of the covariance components can be large and  
13 often negative, indicating ~~that e~~-variability in the sinks (e.g.,  $\sigma_Q^2$ ,  $\sigma_{\Delta S}^2$ ) can, and ~~regularly does~~, exceed variability  
14 in the source ( $\sigma_P^2$ ). Further investigations under extreme conditions revealed that in extremely dry environments  
15 the variance partitioning is closely related to the water storage capacity. With limited storage capacity the  
16 partitioning of  $\sigma_P^2$  is mostly to  $\sigma_E^2$ , but as the storage capacity increases the partitioning of  $\sigma_P^2$  is increasingly  
17 shared between  $\sigma_E^2$ ,  $\sigma_{\Delta S}^2$  and the covariance between those variables. In other environments (i.e., extremely wet  
18 and semi-arid/semi-humid) the variance partitioning proved to ~~be~~ extremely complex and a synthesis ~~was has not~~  
19 ~~been~~ developed. We anticipate that a major scientific effort will be needed to develop a synthesis of hydrologic  
20 variability.

## 22 1. Introduction

23

24 In describing the terrestrial branch of the water cycle, the precipitation ( $P$ ) is partitioned into evapotranspiration  
25 ( $E$ ), runoff ( $Q$ ) and change in water storage ( $\Delta S$ ). With averages taken over many years,  $\overline{\Delta S}$  is usually assumed to  
26 be zero and it has long been recognized that the partitioning of the long-term mean annual precipitation ( $\overline{P}$ )  
27 between  $\overline{E}$  and  $\overline{Q}$  was jointly determined by the availability of both water ( $\overline{P}$ ) and energy (represented by the net  
28 radiation expressed as an equivalent depth of water and denoted  $\overline{E}_o$ ) fluxes. Using data from a large number of  
29 watersheds, Budyko (1974) developed an empirical relation relating the evapotranspiration ratio ( $\overline{E}/\overline{P}$ ) to the  
30 aridity index ( $\overline{E}_o/\overline{P}$ ). The resultant empirical relation and other Budyko-type forms (e.g., Fu, 1981; Choudhury,  
31 1999; Yang et al., 2008, Roderick and Farquhar, 2011; Sposito, 2017) that partition  $P$  between  $E$  and  $Q$  have  
32 proven to be extremely useful in both understanding and characterising the long-term mean annual hydrological  
33 conditions in a given region.

34

35 However, the long-term mean annual hydrologic fluxes rarely occur in any given year. Instead, society must  
36 (routinely) deal with variability around the long-term mean. The classic hydro-climate extremes are droughts and  
37 floods but the key point here is that hydrologic variability is expressed on a full spectrum of time and space scales.  
38 To accommodate that perspective, we need to extend our thinking beyond the long-term mean to ask how the  
39 variability of  $P$  is partitioned into the variability of  $E$ ,  $Q$  and  $\Delta S$  (e.g., Orth and Destouni, 2018).<sup>2</sup>

40

41 Early research on hydrologic variability focussed on extending the Budyko curve. In particular, Koster and Suarez  
42 (1999) used the Budyko curve to investigate analyse inter-annual variability in the water cycle. In their framework,  
43 the evapotranspiration standard deviation ratio (defined as the ratio of standard deviation for  $E$  to  $P$ ,  $\sigma_E/\sigma_P$ ) was  
44 (also) estimated using the aridity index ( $\overline{E}_o/\overline{P}$ ). The classic Koster and Suarez framework has been widely applied  
45 and extended in subsequent investigations of the variability in both  $E$  and  $Q$ , using catchment observations,  
46 reanalysis data and model outputs (e.g., McMahon et al., 2011; Wang and Alimohammadi 2012;  
47 Sankarasubramanian and Vogel, 2002; Zeng and Cai, 2015). However, typical applications of the Koster and  
48 Suarez framework have previously been at regional scales and there is still no comprehensive global assessment  
49 for the partitioning the of variability of  $P$  into the variability of  $E$ ,  $Q$  and  $\Delta S$ . One reason for the lack of a global  
50 comprehensive assessment is the absence of gridded global hydrologic data. Interestingly, the atmospheric science

51 community have long used a combination of observations and model outputs to construct [gridded global-scale](#)  
52 atmospheric re-analyses and such products have become central to atmospheric research. Those atmospheric  
53 products also contain estimates of some of the key water cycle variables (e.g.,  $P$ ,  $E$ ), such as in the widely used  
54 interim ECMWF Re-Analysis (ERA-Interim; Dee et al. 2011). However, the central aim of atmospheric re-  
55 analysis is to estimate atmospheric variables, which, understandably, ignores many of the nuances of soil water  
56 infiltration, vegetation water uptake, runoff generation and many other processes of central importance in  
57 hydrology.

58  
59 Hydrologists have only recently accepted the challenge of developing their own re-analysis type products with  
60 perhaps the first serious hydrologic re-analysis being published as recently as a few years ago (Rodell et al., 2015).  
61 More recently, the Princeton University group has extended this early work by making available a gridded global  
62 terrestrial hydrologic re-analysis product known as the Climate Data Record (CDR) (Zhang et al., 2018). Briefly,  
63 the CDR was constructed by synthesizing multiple in-situ observations, satellite remote sensing products, and  
64 land surface model outputs to provide *gridded* estimates of global land precipitation  $P$ , evapotranspiration  $E$ ,  
65 runoff  $Q$  and total water storage change  $\Delta S$  ( $0.5^\circ \times 0.5^\circ$ , monthly, 1984-2010). In developing the CDR, the authors  
66 adopted local water budget closure as the fundamental hydrologic principle. That approach presented one  
67 important difficulty. Global observations of  $\Delta S$  start with the GRACE satellite mission from 2002. Hence before  
68 2002 there is no direct observational constraint on  $\Delta S$  and the authors made the further assumption that the mean  
69 annual  $\Delta S$  over the full 1984-2010 period was zero at every grid-box. That is incorrect in some regions (e.g.  
70 Scanlon et al., 2018) and represents an observational problem that cannot be overcome. However, our interest is  
71 in the year-to-year variability and for that application, the assumption of no change in the mean annual  $\Delta S$  over  
72 the full 1984-2010 period is unlikely to lead to major problems since we are not looking for subtle changes over  
73 ~~time~~[the full time series](#). With that caveat in mind, the aim of this study is to use this new 27-year gridded  
74 hydrologic re-analysis product to conduct an initial investigation of the inter-annual variability of the terrestrial  
75 branch of the global water cycle.

76  
77 The paper is structured as follows. We begin in Section 2 by describing the various climate and hydrologic  
78 databases including a further assessment of the suitability of the CDR database for this initial variability study. In  
79 Section 3, we examine relationships between the mean and variability in the four water cycle variables ( $P$ ,  $E$ ,  $Q$

80 and  $\Delta S$ ). In Section 4, we first relate the variability to the classical aridity index and then use those results to  
81 evaluate the theory of Koster and Suarez (1999). Subsequently we examine how the variance of  $P$  is partitioned  
82 into the variances (and relevant covariances) of  $E$ ,  $Q$  and  $\Delta S$  and undertake an initial survey that investigates some  
83 of the factors controlling the variance partitioning. We conclude finalise the paper with a discussion summarising  
84 what we have learnt about water cycle variability over land by using the CDR database.

85

## 86 2. Methods and Data

### 87 2.1 Methods

88 The water balance is defined by,

$$89 P(t) = E(t) + Q(t) + \Delta S(t) \quad (1)$$

90 with  $P$  the precipitation,  $E$  the evapotranspiration,  $Q$  the runoff and  $\Delta S$  the total water storage change in time  
91 step  $t$ . By the usual variance law, we have,

$$92 \sigma_P^2 = \sigma_E^2 + \sigma_Q^2 + \sigma_{\Delta S}^2 + 2cov(E, Q) + 2cov(E, \Delta S) + 2cov(Q, \Delta S) \quad (2)$$

93 that includes all relevant variances (denoted  $\sigma^2$ ) and covariances (denoted  $cov$ ). Eq. (1) is the familiar hydrologic  
94 mass balance equation. In that context, Eq. (2) can be thought of as the hydrologic variance balance equation.

95

### 96 2.2 Hydrologic and Climatic Data

97

98 We use the recently released global land hydrologic re-analysis known here as the Climate Data Record (CDR)  
99 (Zhang et al., 2018). This product includes global precipitation  $P$ , evapotranspiration  $E$ , runoff  $Q$  and water storage  
100 change  $\Delta S$  ( $0.5^\circ \times 0.5^\circ$ , monthly, 1984-2010). In this study we focus on the inter-annual variability and the  
101 monthly water cycle variables ( $P$ ,  $E$ ,  $Q$  and  $\Delta S$ ) are aggregated to annual totals. The CDR does not report additional  
102 radiation ve-variables and we use the NASA/GEWEX Surface Radiation Budget (SRB) Release-3.0 (monthly,  
103 1984-2007,  $1^\circ \times 1^\circ$ ) database (Stackhouse et al., 2011) to calculate  $E_o$  (defined as the net radiation expressed as  
104 an equivalent depth of liquid water, Budyko, 1974). We then calculate the aridity index ( $\overline{E_o}/\overline{P}$ ) using  $P$  from the  
105 CDR and  $E_o$  from the SRB databases (see Fig. S1a in the Supplementary Material).

106

107 On general grounds, we anticipate that two important factors likely to influence control the partitioning of  
108 hydrologic variability were the water storage capacity and the presence of ice/snow at the surface. For the storage,

Formatted: Justified, Right: 0.03 cm

109 ~~the active range of the monthly water storage variation was used to approximately we estimate represent~~ the water  
110 storage capacity ( $S_{\max}$ ) ~~in this study using the monthly  $\Delta S$  data in CDR database. In more detail, (~~The water storage  
111  $S(t)$  at each time step  $t$  (monthly here) was first calculated from the accumulation of  $\Delta S(t)$ , i.e.,  $S(t) = S(t-1) + \Delta S(t)$   
112 where we assumed zero storage at the beginning of the study period (i.e.,  $S(0) = 0$ ). With the resulting time series  
113 available,  $S_{\max}$  was estimated as the difference between the maximum and minimum  $S(t)$  during the study period  
114 at each grid-box (see Fig. S1b in the Supplementary Material). The estimated  $S_{\max}$  shows a large range from 0 to  
115 1000 mm with the majority of values from 50 to 600 mm (Fig. S1b), which generally agrees with global rooting  
116 depth estimates assuming that water occupies from 10 to 30% of the soil volume at field capacity (Jackson et al.,  
117 1996; Wang-Erlandsson et al., 2016; Yang et al., 2016). To characterise snow/ice cover, and to distinguish  
118 extremely hot and cold regions, we also make use of a gridded global land air temperature dataset from the  
119 Climatic Research Unit (CRU TS4.01 database, monthly, 1901-2016,  $0.5^\circ \times 0.5^\circ$ ) (Harris et al., 2014). (see Fig.  
120 S1c in the Supplementary Material).

121

### 122 2.3 Spatial Mask to Define Study Extent

123

124 The CDR database provides an estimate of the uncertainty ( $\pm 1\sigma$ ) for each of the hydrologic variables ( $P$ ,  $E$ ,  $Q$ ,  
125  $\Delta S$ ) in each month. We use those uncertainty estimates to identify and remove regions with high relative  
126 uncertainty in the CDR data. The relative uncertainty is calculated as the ratio of root mean square of the  
127 uncertainty ( $\pm 1\sigma$ ) to the mean annual  $P$ ,  $E$  and  $Q$  at each grid-box following the procedure used by Milly and  
128 Dunne (2002a). Note that the long term mean  $\Delta S$  is zero by construction in the CDR database, and for that reason  
129 we did not use  $\Delta S$  to calculate the relative uncertainty. Grid-boxes with a relative uncertainty (in  $P$ ,  $E$  and  $Q$ ) of  
130 more than ~~0.1-10%~~ are deemed to have high relative uncertainty (Milly and Dunne, 2002a) and were excluded  
131 from the study extent. The excluded grid-boxes were mostly in the Himalayan region, the Sahara Desert and in  
132 Greenland. The final spatial mask is shown in ~~Fig. 4~~Fig. S2 and this has been applied throughout this study.

133

### 134 2.4 Further Evaluation of CDR Data for Variability Analysis

135

136 In the original work, the CDR database was validated by comparison with independent observations including (i)  
137 mean seasonal cycle of  $Q$  from 26 large basins (see Fig. 8 in Zhang et al., 2018), (ii) mean seasonal cycle of  $\Delta S$   
138 from 12 large basins (Fig. 10 in Zhang et al., 2018), (iii) monthly runoff from 165 medium size basins and a

139 further 862 small basins (Fig. 14 in Zhang et al., 2018), (iv) summer  $E$  from 47 flux towers (Fig. 16 in Zhang et  
140 al., 2018). Those evaluations did not directly address variability in various water cycle elements. With our focus  
141 on the variability we decided to conduct further validations of the CDR database beyond those described in the  
142 original work. In particular, we focussed on further independent assessments of  $E$  and we use monthly (as opposed  
143 to summer) observations of  $E$  from FLUXNET to evaluate the variability in  $E$ . We also compare the CDR with  
144 two other gridded global  $E$  products that were not used to develop the CDR including [the LandFluxEval database](#)  
145 ( $1^\circ \times 1^\circ$ , monthly, 1989-2005) (Mueller et al., 2013) and the Max Planck Institute [database](#) (MPI,  $0.5^\circ \times 0.5^\circ$ ,  
146 monthly, 1982-2011) (Jung et al., 2010) ~~product~~.

147

148 For the comparison to FLUXNET observations (Baldocchi et al., 2001; Agarwal et al., 2010) we identified 32  
149 flux tower sites (site locations are shown in [Fig. S2Fig. S3](#) and details are shown in Table S1) having at least three  
150 years of continuous (monthly) measurements using the FluxnetLSM R package (v1.0) (Ukkola et al. 2017). The  
151 monthly totals and annual climatology of  $P$  and  $E$  from CDR generally follow FLUXNET observations, with high  
152 correlations and reasonable Root Mean Square Error (Figs. [S4-S5S3-S4](#), Table S1). Comparison of the point-  
153 based FLUXNET (~ 100 m – 1 km scale) with the grid-based CDR (~ 50 km scale) is problematic since the CDR  
154 represents an area that is at least 2500 times larger than the area represented by the individual FLUXNET towers  
155 and we anticipate that the CDR record would be “smoothed” relative to the FLUXNET record. With that in mind,  
156 we chose to compare the ratio of the standard deviation of  $E$  to  $P$  between the CDR and FLUXNET databases and  
157 this normalised comparison of the hydrologic variability proved encouraging ([Fig. S5Fig. S6](#)).

158

159 ~~The comparison of  $E$  between the CDR and the LandFluxEval and MPI databases also proved encouraging. As a~~  
160 ~~further evaluation, we compare gridded  $E$  data in the CDR database against two other global  $E$  databases~~  
161 ~~(including i.e. LandFluxEVAL ( $1^\circ \times 1^\circ$ , monthly, 1989-2005) (Mueller et al., 2013) and Max Planck Institute~~  
162 ~~(MPI),  $0.5^\circ \times 0.5^\circ$ , monthly, 1982-2011) (Jung et al., 2010) that were not used to construct the CDR database. We~~  
163 found that [the](#) monthly mean  $E$  from the CDR database is slightly underestimated compared with LandFluxEVAL  
164 database ([Fig. S6Fig. S7a](#)), but agrees closely with the MPI database ([Fig. S7Fig. S8a](#)). In terms of variability, the  
165 standard deviations of monthly  $E$  from the CDR are [in very close agreement with the LandFluxEVAL database](#)  
166 [\(Fig. S7c\) but there was a bias and scaling offset for the comparison with the MPI database \(Fig. S8c\).](#)

167

Formatted: Font: Italic

168 slightly different than those in the MPI database (Fig. S7Fig. S8c) but were in very close agreement with the  
169 LandFluxEVAL database (Fig. S6Fig. S7c). In summary, we concluded that while the the-CDR database was  
170 unlikely to be perfect, it was nevertheless suitable for an initial exploratory survey investigation of the  
171 inter-annual variability in the terrestrial branch of the global water cycle.

172

### 173 3. Mean and Variability of Water Cycle Components

#### 174 3.1 Mean Annual $P$ , $E$ , $Q$ and the Budyko Curve

175

176 The global pattern of mean annual  $P$ ,  $E$ ,  $Q$  using the CDR data (1984-2007) is shown in Fig. 2Fig. 1. The mean  
177 annual  $P$  ( $\bar{P}$ ) is prominent in tropical regions, southern China, eastern and western North America (Fig. 2Fig. 1a).  
178 The magnitude of mean annual  $E$  ( $\bar{E}$ ) more or less follows the pattern of  $\bar{P}$  in the tropics (Fig. 2Fig. 1b) while the  
179 mean annual  $Q$  ( $\bar{Q}$ ) is particularly prominent in the Amazon, South and Southeast Asia, tropical parts of west  
180 Africa and in some other coastal regions at higher latitudes (Fig. 2Fig. 1c).

181

182 We relate the grid-box level ratio of  $\bar{E}$  to  $\bar{P}$  in the CDR database to the classical Budyko (1974) curve using the  
183 aridity index ( $\bar{E}_o/\bar{P}$ ) (Fig. 3Fig. 2a). As noted previously, in the CDR database,  $\bar{\Delta S}$  is forced to be zero and this  
184 enforced steady state (i.e.,  $\bar{P} = \bar{E} + \bar{Q}$ ) allowed us to also predict the ratio of  $\bar{Q}$  to  $\bar{P}$  using the same Budyko  
185 curve (Fig. 3Fig. 2b). The Budyko curves follow the overall trend in the CDR data, which agrees with previous  
186 studies showing that the dominant effect of aridity index can be used to predict ~~on~~ water availability (e.g.,  
187 Gudmundsson et al., 2016). However, there is substantial scatter due to, for example, regional variations related  
188 to seasonality, water storage change and the physics of runoff generation (Milly, 1994a, b). With that caveat in  
189 mind, the overall patterns are as expected with  $\bar{E}$  following  $\bar{P}$  in dry environments ( $\bar{E}_o/\bar{P} > 1.0$ ) while  $\bar{E}$  follows  
190  $\bar{E}_o$  in wet environments ( $\bar{E}_o/\bar{P} \leq 1.0$ ) (Fig. 3Fig. 2).

191

#### 192 3.2 Inter-annual Variability in $P$ , $E$ , $Q$ and $\Delta S$

193

194 We use the variance balance equation (Eq. 2) to partition the inter-annual  $\sigma_P^2$  into separate components due to  $\sigma_E^2$ ,  
195  $\sigma_Q^2$ ,  $\sigma_{\Delta S}^2$  along with the three covariance components ( $2cov(E, Q)$ ,  $2cov(E, \Delta S)$ ,  $2cov(Q, \Delta S)$ ) (Fig. 4Fig. 3). The  
196 spatial pattern of  $\sigma_P^2$  (Fig. 4Fig. 3a) is very similar to that of  $\bar{P}$  (Fig. 2Fig. 1a), which implies that the  $\sigma_P^2$  is  
197 positively correlated with  $\bar{P}$ . In contrast the partitioning of  $\sigma_P^2$  to the various components is very different from

198 the partitioning of  $\bar{P}$  (cf. [Fig. 2Fig. 1](#) and [43](#)). First we note that while the overall spatial pattern of  $\sigma_E^2$  more or  
199 less follows  $\sigma_P^2$ , the overall magnitude of  $\sigma_E^2$  is much smaller than  $\sigma_P^2$  and  $\sigma_Q^2$  in most regions, and in fact  $\sigma_E^2$  is  
200 also generally smaller than  $\sigma_{\Delta S}^2$ . The prominence of  $\sigma_{\Delta S}^2$  (compared to  $\sigma_E^2$ ) surprised us. The three covariance  
201 components ( $cov(E, Q)$ ,  $cov(E, \Delta S)$ ,  $cov(Q, \Delta S)$ ) are also important in some regions. In more detail, the  
202  $cov(E, Q)$  term is prominent in regions where  $\sigma_Q^2$  is large and is mostly negative in those regions ([Fig. 4Fig. 3e](#)),  
203 indicating that years with lower  $E$  are associated with higher  $Q$  and vice-versa. There are also a few regions with  
204 prominent positive values for  $cov(E, Q)$  (e.g., the seasonal hydroclimates of northern Australia) indicating that in  
205 those regions, years with a higher  $E$  are associated with higher  $Q$ . The  $cov(E, \Delta S)$  term ([Fig. 4Fig. 3f](#)) has a similar  
206 spatial pattern to the  $cov(E, Q)$  term ([Fig. 4Fig. 3e](#)) but with a smaller overall magnitude. Finally, the  $cov(Q, \Delta S)$   
207 term shows a more complex spatial pattern, with both prominent positive and negative values ([Fig. 4Fig. 3g](#)) in  
208 regions where  $\sigma_Q^2$  ([Fig. 4Fig. 3c](#)) and  $\sigma_{\Delta S}^2$  ([Fig. 4Fig. 3d](#)) are both large.

209  
210 These results show that the spatial patterns in variability are not simply a reflection of patterns in the long-term  
211 mean state. On the contrary, we find that of the three primary variance terms, the overall magnitude of (inter-  
212 annual)  $\sigma_E^2$  is the smallest implying the least (inter-annual) variability in  $E$ . This is very different from the  
213 conclusions based on spatial patterns in the mean  $P$ ,  $E$  and  $Q$  (see [previous section 3.1](#)). Further, while  $\sigma_Q^2$  more  
214 or less follows  $\sigma_P^2$  as expected, we were surprised by the magnitude of  $\sigma_{\Delta S}^2$ , which, in general, substantially exceeds  
215 the magnitude of  $\sigma_E^2$ . Further, the magnitude of the covariance terms can be important, especially in regions with  
216 high  $\sigma_Q^2$ . However, unlike the variances, the covariance can be both positive and negative and this introduces  
217 additional complexity. For example, with a negative covariance it is possible for the variance in  $Q$  ( $\sigma_Q^2$ ) to exceed  
218 the variance in  $P$  ( $\sigma_P^2$ ). To examine that in more detail we calculated the equivalent frequency distribution for each  
219 of the plots in [Fig. 4Fig. 3](#). The results ([Fig. 5Fig. S9](#)) further emphasise that in general,  $\sigma_E^2$  is the smallest of the  
220 variances ([Fig. 5Fig. S9b](#)). We also note that the frequency distributions for the covariances ([Fig. 5Fig. S9efg](#)) are  
221 not symmetrical. In summary, it is clear that spatial patterns in the inter-annual variability of the water cycle ([Fig.](#)  
222 [4Fig. 3](#)) do not simply follow the spatial patterns for the inter-annual mean ([Fig. 2Fig. 1](#)).

### 224 3.3 Relation Between Variability and the Mean State for $P$ , $E$ , $Q$

226 Differences in the spatial patterns of the mean (Fig. 2Fig. 1) and inter-annual variability (Fig. 4Fig. 3) in the global  
227 water cycle led us to further investigate the relation between the mean and the variability for each separate  
228 component. Here we relate the standard deviation ( $\sigma_P$ ,  $\sigma_E$ ,  $\sigma_Q$ ) instead of the variance to the mean of each water  
229 balance flux (Fig. 6Fig. 4) since the standard deviation has the same physical units as the mean making the results  
230 more comparable. As inferred previously, we find  $\sigma_P$  to be positively correlated with  $\bar{P}$  but with substantial scatter  
231 (Fig. 6Fig. 4a). The same result more or less holds for the relation between  $\sigma_Q$  and  $\bar{Q}$  (Fig. 6Fig. 4c). In contrast  
232 the relation between  $\sigma_E$  and  $\bar{E}$  is very different (Fig. 6Fig. 4b). In particular,  $\sigma_E$  is a small fraction of  $\bar{E}$  and this  
233 complements the earlier finding (Fig. 6Fig. 4b) that the inter-annual variability for  $E$  is generally smaller than for  
234 the other physical variables, ( $P$ ,  $Q$  and  $\Delta S$ ). (The same result was also found using both LandFluxEVAL and  
235 MPI databases, see Fig. S8Fig. S10 in the Supplementary Material.) Importantly, unlike  $P$  and  $Q$ ,  $E$  is constrained  
236 by both water and energy availability (Budyko, 1974) and the limited inter-annual variability in  $E$  presumably  
237 reflects limited inter-annual variability in the available (radiant) energy ( $E_o$ ). This is something that could be  
238 investigated in a future study.

239

#### 240 4. Relating the Variability of Water Cycle Components $P$ , $E$ , $Q$ and $\Delta S$ to Aridity

241

242 In the previous section, we investigated spatial patterns of the mean and the variability in the global water cycle.  
243 In this section, we extend that by investigating the partitioning of  $\sigma_P^2$  to the three primary physical terms ( $\sigma_E^2$ ,  $\sigma_Q^2$ ,  
244  $\sigma_{\Delta S}^2$ ) along with the three relevant covariances. For that, we begin by comparing the Koster and Suarez (1999)  
245 theory against the CDR data and then investigate how the partitioning of the variance is related to the aridity index  
246  $\bar{E}_o/\bar{P}$  (see Fig. S1a in the Supplementary Material). Following that, we investigate variance partitioning in relation  
247 to both our estimate of the storage capacity  $S_{\max}$  (see Fig. S1b in the Supplementary Material) as well as the mean  
248 annual air temperature  $\bar{T}_a$  (see Fig. S1c in the Supplementary Material) that we use as a surrogate for snow/ice  
249 cover. We finalise this section by examining the partitioning of variance at three selected study sites that represent  
250 extremely dry/wet, high/low water storage capacity and the hot/cold spectrums.

251

##### 252 4.1 Comparison with the Koster and Suarez (1999) Theory

253

254 We first evaluate the classical empirical curve of Koster and Suarez (1999) by relating ratios  $\sigma_E/\sigma_P$  and  $\sigma_E/\sigma_P$  to  
255 the aridity index (Fig. 7Fig. 5). The ratio  $\sigma_E/\sigma_P$  in the CDR database is generally overestimated by the empirical

Formatted: Font: Not Italic

256 Koster and Suarez curve, especially in dry environments (e.g.,  $\overline{E_o}/\overline{P} > 3$ ) (Fig. 5a). The inference here is that the  
257 Koster and Suarez theory predicts  $\sigma_E/\sigma_P$  to approach unity in dry environments while the equivalent value in the  
258 CDR data is occasionally unity but is generally smaller. With  $\sigma_E/\sigma_P$  generally overestimated by the Koster and  
259 Suarez theory we expect, and find, that  $\sigma_Q/\sigma_P$  is generally underestimated by the same theory (Fig. 7Fig. 5b). The  
260 same overestimation was found based on the other two independent databases for  $E$  (LandFluxEVAL and MPI)  
261 (Fig. S9Fig. S11). This overestimation is discussed further in section 5.

#### 263 4.2 Relating Inter-annual Variability to Aridity

264  
265 Here we examine how the fraction of the total variance in precipitation accounted for by the three primary variance  
266 terms along with the three covariance terms varies with the aridity index ( $\overline{E_o}/\overline{P}$ ) (Fig. 8Fig. 6). (Also see Fig.  
267 S10Fig. S12 for the spatial maps.) The ratio  $\sigma_E^2/\sigma_P^2$  is close to zero in extremely wet regions and has an upper  
268 limit noted previously (Fig. 7Fig. 5a) that approaches unity in extremely dry regions (Fig. 8Fig. 6a). The ratio  
269  $\sigma_Q^2/\sigma_P^2$  is close to zero in extremely dry regions but approaches unity in extremely wet regions but with substantial  
270 scatter (Fig. 8Fig. 6b). The ratio  $\sigma_{\Delta S}^2/\sigma_P^2$  is close to zero in both extremely dry/wet regions (Fig. 8Fig. 6c) and but  
271 shows the largest range at an intermediate aridity index ( $\overline{E_o}/\overline{P} \sim 1.0$ ).

272  
273 The covariance ratios are all small in extremely dry (e.g.,  $\overline{E_o}/\overline{P} \geq 6.0$ ) environments and generally show the largest  
274 range in semi-arid and semi-humid environments. The peak magnitudes for the three covariance components  
275 consistently occur when  $\overline{E_o}/\overline{P}$  is close to 1.0 which is the threshold often used to separate wet and dry  
276 environments.

#### 278 4.3 Further Investigations on the Factors Controlling Partitioning of the Variance

279  
280 Results in the previous section results (Sections 4.1 and 4.2) have demonstrated that spatial variation in the  
281 partitioning of  $\sigma_P^2$  into  $\sigma_E^2$ ,  $\sigma_Q^2$ ,  $\sigma_{\Delta S}^2$  and the three covariance components is complex (Fig. 6). To help further  
282 understand inter-annual variability of the terrestrial water cycle, we conduct further investigations in this section  
283 using two factors likely to have a major influence on the variance partitioning of  $\sigma_P^2$ . The first is the storage  
284 capacity  $S_{\max}$  (see Fig. S1b in the Supplementary Material). The second is the mean annual air temperature  $\overline{T_a}$  (see  
285 Fig. S1c in the Supplementary Material) which is used here as a surrogate for snow/ice presence.

286

#### 287 4.3.1 Relating Inter-annual Variability to Storage Capacity

288

289 We first relate the partitioning of  $\sigma_p^2$  to water storage capacity ( $S_{\max}$ ) by repeating Fig. 8 Fig. 6 but instead we use  
290 a logarithmic scale for the x-axis and we distinguish  $S_{\max}$  via the background colour (Fig. 9 Fig. 7). To eliminate  
291 the possible overlap of grid-cells in the colouring process, all the grid-cells over land are further separated using  
292 different latitude ranges (as shown in the four columns of Fig. 9 Fig. 7), i.e., 90N-60N, 60N-30N, 30N-0 and 0-  
293 90S. We find that  $S_{\max}$  is relatively high in wet environments ( $\overline{E_o}/\overline{P} \leq 1.0$ , Fig. 7a) but shows no obvious relation  
294 to with the partitioning of  $\sigma_p^2$ . However, in dry environments ( $\overline{E_o}/\overline{P} > 1.0$ ) the ratio  $\sigma_E^2/\sigma_p^2$  apparently decreases  
295 with the increase of  $S_{\max}$  (Fig. 9 Fig. 7a-d). That relation is particularly obvious in extremely dry environments  
296 ( $\overline{E_o}/\overline{P} \geq 6.0$ ) at equatorial latitudes where there is an upper limit of  $\sigma_E^2/\sigma_p^2$  close to 1.0 when  $S_{\max}$  is small (blue  
297 grid-cells in Fig. 9 Fig. 7c). The interpretation for those extremely dry environments is that when  $S_{\max}$  is small,  $\sigma_p^2$   
298 is almost completely partitioned into  $\sigma_E^2$  (Fig. 9 Fig. 7bc) with the other variance and covariance components close  
299 to zero. While for those same extremely dry environments, as  $S_{\max}$  increases, the partitioning of  $\sigma_p^2$  is shared  
300 between  $\sigma_E^2$  and  $\sigma_{\Delta S}^2$  and their covariance (Fig. 9 Fig. 7cks) while  $\sigma_Q^2$  and its covariance components remain  
301 close to zero (Fig. 9 Fig. 7gow). However, at polar latitudes in the northern hemisphere (panels in the first and  
302 second columns of Fig. 9 Fig. 7) there are variations that could not be easily associated with variations in  $S_{\max}$   
303 which led us to further investigate the role of snow/ice on the variance partitioning in the following section.

304

#### 305 4.3.2 Relating Inter-annual Variability to Mean Air Temperature

306

307 To understand the potential role of snow/ice in modifying the variance partitioning, we repeat the previous  
308 analysis (Fig. 9 Fig. 7) but here we use the mean annual air temperature ( $\overline{T_a}$ ) to colour the grid-cells to (crudely)  
309 indicate ~~identify~~ the presence of snow/ice (Fig. 10 Fig. 8). The results are complex and not easy to simply  
310 understand. The most important difference revealed by this analysis is in the hydrologic partitioning between cold  
311 (first column) and hot (third column) conditions in wet environments ( $\overline{E_o}/\overline{P} \leq 0.5$ ). In particular, when  $\overline{T_a}$  is high,  
312  $\sigma_p^2$  is almost completely partitioned into  $\sigma_Q^2$  in wet environments (e.g.,  $\overline{E_o}/\overline{P} \leq 0.5$ , Fig. 8g). In contrast, when  $\overline{T_a}$   
313 is low in a wet environment ( $\overline{E_o}/\overline{P} \leq 0.5$  in first column of Fig. 8), there are substantial variations in the  
314 hydrologic partitioning. That result reinforces the complexity of variance partitioning in the presence of snow/ice.

315 Most of the variations at polar latitudes in the northern hemisphere (panels in the first and second columns of Fig.  
 316 10Fig. 8) is associated with low air temperature (e.g.,  $\overline{T_a} < 0^\circ\text{C}$  in blue colour), making the results associated with  
 317 high air temperature (e.g.,  $\overline{T_a} > 10^\circ\text{C}$  in the third and fourth columns of Fig. 8green-yellow-red colours) relatively  
 318 more compactshow less scatters. That pattern is particularly obvious in extremely wet environment ( $\overline{E_o}/\overline{P} \leq 0.5$ ),  
 319 where the ratio  $\sigma_Q^2/\sigma_P^2$  is close to 1.0 when  $\overline{T_a}$  is high (e.g.,  $\overline{E_o}/\overline{P} \leq 0.5$  and  $\overline{T_a} > 10^\circ\text{C}$ , with green-yellow-red  
 320 grid-cells on the panels in the second row of Fig. 10Fig. 8gh) but shows lots of scatters when  $\overline{T_a}$  is low (e.g.,  $\overline{T_a}$   
 321  $< 0^\circ\text{C}$ , Fig. 8ef)with the other variance-covariance components close to zero. This indicates that in extremely wet  
 322 environment, when  $\overline{T_a}$  is high,  $\sigma_P^2$  is almost completely partitioned into  $\sigma_Q^2$  (e.g.,  $\overline{E_o}/\overline{P} \leq 0.5$  and  $\overline{T_a} > 10^\circ\text{C}$  in the  
 323 third and fourth columns of Fig. 8). However, when  $\overline{T_a}$  is low in extremely wet environment, there are substantial  
 324 variations in all variance-covariance components (e.g.,  $\overline{E_o}/\overline{P} \leq 0.5$  and  $\overline{T_a} < 0^\circ\text{C}$ , see the blue grid-cells on the  
 325 panels in the first and second columns column of Fig. 10Fig. 8). That result indicates the complexity of variance  
 326 partitioning associated with the presence of snow/ice.

327

#### 328 4.4 Case Studies

329

330 The previous results (Section 4.3) have demonstrated that the partitioning of  $\sigma_P^2$  is predominantly influenced by  
 331 the water storage capacity ( $S_{\max}$ ) in extremely dry environments ( $\overline{E_o}/\overline{P} \geq 6.0$ ) and that the presence of snow/ice is  
 332 important (as indicated by mean air temperature ( $\overline{T_a}$ )) in extremely wet environments ( $\overline{E_o}/\overline{P} \leq 0.5$ ). In this section,  
 333 we examine, in greater detail, several sites to gain deeper understanding of the partitioning of  $\sigma_P^2$ . For that purpose,  
 334 we selected three sites based on extreme values for the three explanatory parameters, i.e.,  $\overline{E_o}/\overline{P}$  (Fig. S1a),  $S_{\max}$   
 335 (Fig. S1b) and  $\overline{T_a}$  (Fig. S1c). The criteria to select three climate sites are as follows, Site 1: dry ( $\overline{E_o}/\overline{P} \geq 6.0$ ) and  
 336 small  $S_{\max}$  ( $S_{\max} \approx 0$ ), Site 2: dry ( $\overline{E_o}/\overline{P} \geq 6.0$ ) and relatively large  $S_{\max}$  ( $S_{\max} \gg 0$ ) and Site 3: wet ( $\overline{E_o}/\overline{P} \leq 0.5$ )  
 337 and hot ( $\overline{T_a} > 25^\circ\text{C}$ ). For each of the three classes, sites, we use a representative grid-cell (Fig. 14Fig. 9) to show  
 338 the original time series (Fig. 12Fig. 10) and the partitioning of the variability (Fig. 13Fig. 11).

339

340 We show the  $P$ ,  $E$ ,  $Q$  and  $\Delta S$  time series along with the relevant variances and covariances in Fig. 12Fig. 10.  
 341 Starting with the two dry sites, at the site with low storage capacity (Site 1), the time series shows that  $E$  closely  
 342 follows  $P$  leaving annual  $Q$  and  $\Delta S$  close to zero (Fig. 12Fig. 10a). The variance of  $P$  ( $\sigma_P^2 = 206.9 \text{ mm}^2$ ) is small  
 343 and almost completely partitioned into the variance of  $E$  ( $\sigma_E^2 = 196.9 \text{ mm}^2$ ), leaving very limited variance for  $Q$ ,  
 344  $\Delta S$  and all three covariance components (Fig. 12Fig. 10b). At the dry site with larger high-storage capacity (Site

Formatted: Font: 10 pt, Not Italic

Formatted: Font: 10 pt

Formatted: Font: 10 pt

Formatted: Font: 10 pt

Formatted: Font: 10 pt

Formatted: Font: 10 pt

Formatted: Font: 10 pt, Not Italic

Formatted: Font: 10 pt, Not Italic

Formatted: Font: 10 pt, Not Italic

Formatted: Font: 10 pt, Not Italic

345 2),  $E$ ,  $Q$  and  $\Delta S$  do not simply follow  $P$  (Fig. 12Fig. 10c). As a consequence, the variance of  $P$  ( $\sigma_P^2 = 2798.0 \text{ mm}^2$ )  
 346 is shared between  $E$  ( $\sigma_E^2 = 1150.2 \text{ mm}^2$ ),  $\Delta S$  ( $\sigma_{\Delta S}^2 = 800.5 \text{ mm}^2$ ) and their covariance component ( $2cov(E, \Delta S) =$   
 347  $538.4 \text{ mm}^2$ , Fig. 12Fig. 10d). Switching now to the remaining wet and hot site (Site 3), we note that  $Q$  closely  
 348 follows  $P$ , with  $\Delta S$  close to zero and  $E$  showing little inter-annual variation (Fig. 12Fig. 10e). The variance of  $P$   
 349 ( $\sigma_P^2 = 57374.4 \text{ mm}^2$ ) is relatively large and almost completely partitioned into the variance of  $Q$  ( $\sigma_Q^2 = 57296.4$   
 350  $\text{mm}^2$ ), leaving very limited variance for  $E$  and  $\Delta S$  and the three covariance components (Fig. 12Fig. 10f). We also  
 351 examined numerous other sites with similar extreme conditions as the three case study sites and found the same  
 352 basic patterns as reported above.

353  
 354 To put the data from the three case study sites into a broader variability context we position the site data onto a  
 355 backdrop of original Fig. 8Fig. 6. As noted previously, at Site 1, the ratio  $\sigma_E^2/\sigma_P^2$  is very close to unity (Fig. 13Fig.  
 356 11a), and under this extreme condition, we have the following approximation,

$$357 \quad \sigma_P^2 \approx \sigma_E^2 \quad (\text{Site 1, dry and } S_{\max} \approx 0) \quad (3)$$

358 In contrast, for Site 2 with the same aridity index but higher  $S_{\max}$ , we have,

$$359 \quad \sigma_P^2 \approx \sigma_E^2 + \sigma_{\Delta S}^2 + 2cov(E, \Delta S) \quad (\text{Site 2, dry and } S_{\max} \gg 0) \quad (4)$$

360 Finally, at Site 3, we have,

$$361 \quad \sigma_P^2 \approx \sigma_Q^2 \quad (\text{Site 3, wet and hot}) \quad (5)$$

362

#### 363 4.5 Synthesis

364

365 The above simple examples demonstrate that aridity  $\overline{E_o}/\overline{P}$ , storage capacity  $S_{\max}$  and to a lesser extent, air  
 366 temperature  $T_{a-1}$ , all play some role roles in the partitioning of  $\sigma_P^2$  to the various components. Our synthesis of the  
 367 results for the partitioning of  $\sigma_P^2$  is summarised in Fig. 14Fig. 12. In dry environments with and low storage  
 368 capacity ( $S_{\max} \approx 0$ ) environments we have minimal runoff and expect that  $\sigma_P^2$  is more or less completely partitioned  
 369 into  $\sigma_E^2$  (Fig. 14Fig. 12a). In those environments, (inter-annual) variations in storage  $\sigma_{\Delta S}^2$  play a limited role in  
 370 setting the overall variability. However, in dry environments with larger storage capacity (and  $S_{\max} \gg 0$ )  
 371 environments,  $\sigma_E^2$  is only a small fraction of  $\sigma_P^2$  (Fig. 12a) leaving most of the overall variance in  $\sigma_P^2$  to be  
 372 partitioned attributed to  $\sigma_{\Delta S}^2$  and the covariance between  $E$  and  $\Delta S$  (Fig. 14Fig. 12c and Fig. 14Fig. 12e). This  
 373 emphasises implies the hydrological importance of water storage capacity in buffering variations of the water  
 374 cycle under dry conditions.

375  
376 Under extremely wet conditions, the ~~largest huge~~ difference in variance partitioning ~~is not due to differences in~~  
377 ~~storage capacity but is instead related to differences in mean air temperature, occurs between the hot and cold~~  
378 ~~conditions instead of water storage capacity conditions in dry conditions environments.~~ In wet and hot  
379 environments, we have maximum runoff and ~~find expect~~ that  $\sigma_p^2$  is more or less completely partitioned into  $\sigma_Q^2$   
380 (Fig. 14 Fig. 12b) ~~while the partitioning to , and the variations in evapotranspiration  $\sigma_E^2$  and storage  $\sigma_{\Delta S}^2$  is small.~~  
381 ~~play a limited role in setting the overall variability.~~ However, in wet and cold environments, the variance  
382 partitioning shows great complexity ~~with  $\sigma_p^2$  being partitioned into all possible components. , with  $\sigma_Q^2/\sigma_P^2$  and~~  
383  ~~$\sigma_{\Delta S}^2/\sigma_P^2$  vary a lot caused by snow/ice melting. We suggest that this emphasises This signifies~~ the hydrological  
384 importance of thermal processes (melting/freezing) under extremely cold conditions.

385  
386 ~~However. t~~The most complex patterns to interpret are those for semi-arid to semi-humid environments (i.e.,  
387  $\bar{E}_0/\bar{P} \sim 1.0$ ). ~~Despite a multitude of attempts over an extended period we were unable to develop a simple useful~~  
388 ~~synthesis to summarise the partitioning of variability in those environments. We found In those environments,~~  
389 ~~that~~ the three covariance terms all play important roles and we ~~also~~ found that simple environmental gradients  
390 (e.g., dry/wet, high/low storage capacity, hot/cold) could not easily explain the observed patterns. ~~We anticipate~~  
391 ~~that vegetation related processes (e.g., phenology, rooting depth, gas exchange characteristics, disturbance, etc.)~~  
392 ~~may prove to be important in explaining hydrologic variability in these biologically productive regions that~~  
393 ~~support most of human population. This result implies that a A-major scientific effort will be needed to develop a~~  
394 ~~synthesis of iseover~~ the controlling factors for variability of the water cycle in these environments.

## 395 396 **5. Discussion and Conclusions**

397  
398 In this study, we have used a recently released global gridded hydrologic re-analysis product, i.e., the Climate  
399 Data Record (CDR) to conduct an initial investigation of inter-annual variability in the terrestrial branch of the  
400 global water cycle. To the best of our knowledge, the results in our manuscript present the first attempt to gain a  
401 global overview of the magnitude for various terms (Eq. 2) that document variability in the water cycle. Our  
402 results demonstrate that the global patterns of inter-annual variability in the water cycle do not simply follow  
403 those of the long-term mean. In particular, with the variance calculations, the annual anomalies are squared and  
404 hence do not cancel out (like they do when calculating the mean). Hence we were initially surprised that the inter-

405 annual variability of water storage change ( $\sigma_{\Delta S}^2$ ) is typically larger than the inter-annual variability of  
406 evapotranspiration ( $\sigma_E^2$ ). Moreover, the covariance components are also prominent and can be negative, which  
407 means that it is possible for the variability in the sinks (e.g.,  $\sigma_Q^2$ ,  $\sigma_{\Delta S}^2$ ) can actually exceed the variability in the  
408 source ( $\sigma_P^2$ ) (Eq. 2).

409  
410 Our further analysis based on six climate end members, dry/wet, high/low water storage capacity and hot/cold  
411 offered some further general insights about hydrologic variability. For example, under extremely dry (water-  
412 limited) conditions, with limited storage capacity ( $S_{\max}$ ) we found that  $E$  follows  $P$  and  $\sigma_E^2$  follows  $\sigma_P^2$ , with  $\sigma_Q^2$   
413 and  $\sigma_{\Delta S}^2$  approaching zero. However, as  $S_{\max}$  increases, the partitioning of  $\sigma_P^2$  progressively shifts to a balance  
414 between  $\sigma_E^2$ ,  $\sigma_{\Delta S}^2$  and  $\text{cov}(E, \Delta S)$  (Fig. 12 Figs. 10-12-14). Under extremely wet (energy-limited) and hot  
415 environments (i.e., no snow/ice impact) we found the inter-annual variations in  $P$  mostly be partitioned to inter-  
416 annual variations in  $Q$  (with both  $\sigma_E^2$  and  $\sigma_{\Delta S}^2$  approaching zero). However, in wet environments that were cold,  
417 we expected thermal processes (freeze/melt) to play a critical role in the hydrologic variability. Our results confirm  
418 that, with the finding that hydrologic partitioning of variability was highly (spatially) variable under extremely  
419 cold conditions (Figs. 10-12-14) and we were unable to provide any useful simplifications to summarise the  
420 data. These results highlight a key point that while the long-term mean state is not especially sensitive to variations  
421 in hydrologic water storage or phase, the long-term variability is very sensitive to those same variations.

422  
423 The most complex results were found in semi-arid/semi-humid ( $0.5 < \overline{E_o}/\overline{P} < 1.5$ ) environments, where all three  
424 covariances (Eq. 2) were found to play critical roles in the overall partitioning of variability (Figs. 3 and Fig. S94-  
425 5). In many regions, the (absolute) magnitudes of the covariances were actually larger than the variances of the  
426 water balance components  $E$ ,  $Q$  and  $\Delta S$  (e.g., Fig. 8 Fig. 6). That result demonstrates that deeper understanding of  
427 the process-level interactions that are embedded within each of the three covariance terms is still needed to help  
428 understand variability in the water cycle in these biologically productive regions ( $0.5 < \overline{E_o}/\overline{P} < 1.5$ ).

429  
430 This study should be viewed as an initial investigation of the inter-annual variability in the global land water cycle.  
431 We managed to obtain some syntheses based on the availability of current data, and we expect that with the  
432 improvement of hydrologic databases over the coming years some of the detailed spatial patterns may change.  
433 However, even from this initial investigation, some general principles do already appear clear. One general finding  
434 is that the global pattern in the partitioning of inter-annual variability in the water cycle is not simply a reflection

435 of patterns in the partitioning of the long-term mean. For example, while the inter-annual water storage change is  
436 often (safely) assumed to be negligible in terms of the long-term mean state, it is clear that storage variations are  
437 central to understanding inter-annual variability of global water cycle. A second generalisation is that the  
438 covariance components (Eq. 2) can be relatively large and are negative in some regions. The consequence is that  
439 variability in the sinks (e.g.,  $\sigma_{\Delta S}^2$ ,  $\sigma_{\Delta Q}^2$ ) can, and do, exceed the variability in the source ( $\sigma_P^2$ ), especially in  
440 biologically productive regions (Fig. 4 Fig. 3).

441  
442 The syntheses of the long-term mean water cycle originated in 1970s (Budyko, 1974), and it took several decades  
443 for those general principles to become widely adopted in the hydrologic community. It remains a challenge to  
444 develop a synthesis of hydro-climatic variability in the terrestrial branch of the water cycle, and major intellectual  
445 efforts will be needed to develop generally applicable principles.

## 447 6. Conclusions

448  
449 Importantly, hydrologists have long been interested in hydrologic variability aware that the water storage effects  
450 were going to be important for understanding water cycle variability (e.g., Milly and Dunne, 2002b; Zhang et al.,  
451 2008; Donohue et al., 2010; Wang and Alimohammadi, 2012), but without readily available databases it has been  
452 difficult to quantify water cycle variability in a consistent way. For example, we are not aware of maps showing  
453 global spatial patterns in variance for any terms of the water balance (except for  $P$ ). In this study, we describe an  
454 initial investigation of the inter-annual variability of the terrestrial branch in the global water cycle that uses the  
455 recently released global monthly Climate Data Record (CDR) database for  $P$ ,  $E$ ,  $Q$  and  $\Delta S$ . We start by  
456 investigating the partitioning of  $P$  in the water cycle in terms of long-term mean and then extend that to the inter-  
457 annual variability. The CDR is one of the first dedicated hydrologic reanalysis databases and includes data for a  
458 27-year period. Accordingly, we could only examine hydrologic variability over this relatively short period.  
459 Further, we expect future improvements and modifications as the hydrologic community seeks to further develop  
460 and refine these new reanalysis databases. With those caveats in mind, we started this analysis –by first  
461 investigating the partitioning of  $P$  in the water cycle in terms of long-term mean and then extended –that to the  
462 inter-annual variability using a theoretical variance balance equation (Eq. 2). Despite the ~~From this~~ initial nature  
463 of this investigation we have been able to establish some useful general principles.

465 The mean annual  $P$  is mostly partitioned into mean annual  $E$  and  $Q$ , as is well known, and the results using the  
 466 CDR were generally consistent with the earlier ~~previous-Budyko framework work~~ (Fig. 2). Having established  
 467 that, the first general finding is that the spatial pattern in the partitioning of inter-annual variability in the water  
 468 cycle is not simply a reflection of the spatial pattern in the partitioning of the long-term mean. In particular, with  
 469 the variance calculations, the annual anomalies are squared and hence the storage anomalies do not cancel out like  
 470 they do when calculating the mean. With that in mind, ~~w~~e were ~~initially~~ surprised that the inter-annual  
 471 variability of water storage change ( $\sigma_{\Delta S}^2$ ) is typically larger than the inter-annual variability of evapotranspiration  
 472 ( $\sigma_E^2$ ) (cf. Fig. 3b and 3d). The consequence is that  $\sigma_{\Delta S}^2$  is more important than  $\sigma_E^2$  for understanding inter-annual  
 473 variability of global water cycle. A second important generalisation is that unlike the variance components which  
 474 are all positive, the three covariance components in the theory (Eq. 2) can be both positive and negative. We report  
 475 results here showing both large positive and negative values for the three covariance terms ~~can be relatively large~~  
 476 ~~and are negative in some regions~~ (Fig. 3efg). The consequence is that variability in the sinks (e.g.,  $\sigma_Q^2, \sigma_{\Delta S}^2$ ) ~~can~~  
 477 ~~and do, exceed the variability in the source~~ ( $\sigma_P^2$ ) This was especially, ~~especially~~ prevalent in biologically  
 478 productive regions ( $0.5 < \overline{E}_o / \overline{P} < 1.5$ , Fig. 3eg). When examining the mean state, we are accustomed to think that  $P$   
 479 sets a limit to  $E$ ,  $Q$  and  $\Delta S$ , as per the mass balance (Eq. 1). But the same thinking does not extend to the variance  
 480 balance since the covariance terms on the right hand side of Eq. 2 can be both large and negative leading to  
 481 circumstances where the variability in the sinks ( $\sigma_E^2, \sigma_Q^2, \sigma_{\Delta S}^2$ ) could actually exceed variability in the source ( $\sigma_P^2$ ).  
 482  
 483 ~~Our initial attempt to develop deeper understanding of variance partitioning was based on a series of case studies~~  
 484 ~~located in extreme environments (wet/dry vs hot/cold vs high/low water storage capacity). The results offered~~  
 485 ~~some further insights about hydrologic variability. For example, under extremely dry (water-limited)~~  
 486 ~~environments, with limited storage capacity ( $S_{\max}$ ) we found that  $E$  follows  $P$  and  $\sigma_E^2$  follows  $\sigma_P^2$ , with  $\sigma_Q^2$  and  $\sigma_{\Delta S}^2$~~   
 487 ~~both approaching zero. However, as  $S_{\max}$  increases, the partitioning of  $\sigma_P^2$  progressively shifts to a balance between~~  
 488  ~~$\sigma_E^2, \sigma_{\Delta S}^2$  and  $\text{cov}(E, \Delta S)$  (Figs. 10-12). This result explains the overestimation of  $\sigma_E / \sigma_P$  by the empirical theory of~~  
 489 ~~Koster and Suarez (1999) which implicitly assumed no inter-annual change in storage. ~~negligible storage variation.~~~~  
 490 ~~The Koster and Suarez ~~at~~ empirical theory is perhaps better described as an upper limit that is based on minimal~~  
 491 ~~storage capacity, and that any increase in storage capacity would promote the partitioning of  $\sigma_P^2$  to  $\sigma_{\Delta S}^2$ , particularly~~  
 492 ~~under dry conditions (Figs. 10-12).~~

494 ~~In Under~~ extremely wet/hot environments (i.e., no snow/ice presence~~impact~~) we found  $\sigma_P^2$  to be mostly partitioned  
495 to  $\sigma_Q^2$  (with both  $\sigma_E^2$  and  $\sigma_{\Delta S}^2$  approaching zero, Fig. 10). In contrast, in ~~under~~ extremely wet/cold environments,  
496 ~~conditions,~~ the partitioning of  $\sigma_P^2$  was highly (spatially) variable presumably because of ~~the~~ spatial variability in  
497 the all-important thermal processes (freeze/melt). These results highlight a key point that while the long-term  
498 mean state is not especially sensitive to variations in either water storage or physical phase (liquid/solid), the  
499 overall hydrologic variability is expected to be sensitive to those same variations.

500  
501 The most complex results were found in mesic biologically productive environments ( $0.5 < \bar{E}_o / \bar{P} < 1.5$ ), where all  
502 three covariance terms (Eq. 2) were found to be relatively large and therefore they all played critical roles in the  
503 overall partitioning of variability (Fig. 6). As noted above, in ~~In~~ many of these regions, the (absolute) magnitudes  
504 of the covariances were actually larger than the variances of the water balance components  $E$ ,  $Q$  and  $\Delta S$  (e.g., Fig.  
505 3). That result demonstrates that deeper understanding of the process-level interactions that are embedded within  
506 each of the three covariance terms (e.g., for instance, the role of seasonal vegetation variation) will be needed to  
507 develop process-based understanding of variability in the water cycle in these biologically productive regions  
508 ( $0.5 < \bar{E}_o / \bar{P} < 1.5$ ).

509  
510 The syntheses of the long-term mean water cycle originated in 1970s (Budyko, 1974), and it took several decades  
511 for those general principles to become widely adopted in the hydrologic community. The hydrologic data needed  
512 to understand hydrologic variability are only now becoming available. With those data we can begin to develop a  
513 process-based understanding of hydrologic variability that can be used for a variety of purposes, e.g., deeper  
514 understanding of such as hydrologic water risk analysis, hydro-climatic behaviour, hydrologic risk analysis,  
515 climate change assessments and hydrologic sensitivity studies are just a few applications that spring to mind. The  
516 initial results presented here show that a major ~~Major~~ intellectual efforts will be needed ~~are still needed~~ to develop  
517 a general understanding of hydrologic variability.

518 ~~We start by investigating the partitioning of  $P$  in the water cycle in terms of long-term mean and then extend~~  
519 ~~that to the inter-annual variability.~~ While the mean annual  $P$  is mostly partitioned into mean annual  $E$  and  $Q$ , as  
520 is well known. However, we find that the variance of  $P$  ( $\sigma_P^2$ ) is mostly partitioned into the variance of  $Q$  ( $\sigma_Q^2$ ) and  
521 variance of  $\Delta S$  ( $\sigma_{\Delta S}^2$ ). This result indicates that the global patterns of inter-annual variability in the water cycle do  
522 not simply follow the long-term mean. A second general finding is that the covariance components are important

523 and can be negative in some regions, indicating the variability in the sinks (e.g.,  $\sigma_Q^2$ ,  $\sigma_{\Delta X}^2$ ) can, and do, exceed the  
524 variability in the source ( $\sigma_P^2$ ). Our attempts to develop deeper understanding of variance partitioning led to some  
525 syntheses in extreme environments (wet/dry vs hot/cold). In particular, we find that in extremely dry environments  
526 (either hot/cold) the partitioning of  $\sigma_P^2$  is closely related to the water storage capacity. With limited storage  
527 capacity, the partitioning of  $\sigma_P^2$  is mostly to  $\sigma_Q^2$  but as the storage capacity increases, the partitioning of  $\sigma_P^2$  is  
528 increasingly shared between  $\sigma_Q^2$  and  $\sigma_{\Delta X}^2$  and the covariance between those variables (Fig. 14 Fig. 12). In contrast,  
529 in extremely wet environments, there are large divergences in the variance partitioning between hot and cold  
530 conditions. In hot conditions,  $\sigma_P^2$  is mostly partitioned to  $\sigma_Q^2$  but under cold conditions,  $\sigma_P^2$  is partitioned to all  
531 available variability sinks (Fig. 14 Fig. 12). However, in biologically productive semi arid/semi humid  
532 ( $0.5 < \overline{E_g}/\overline{P} < 1.5$ ) environments, we found the variance partitioning to be very complex and that partitioning was  
533 not obviously associated with simple environmental factors. A general understanding of hydro-climatic variability  
534 remains a major intellectual challenge and we anticipate major efforts will be needed to synthesise general  
535 principles that cover the full spectrum of hydrologic variability.

#### 536 537 **Acknowledgements**

538 This research was supported by the Australian Research Council (CE11E0098, CE170100023), and D.Y. also  
539 acknowledges support by the National Natural Science Foundation of China (51609122). We thank Dr Anna  
540 Ukkola for help in accessing the FLUXNET database. We thank the reviewers (including Dr René Orth and two  
541 anonymous reviewers) for helpful comments that improved the manuscript. The authors declare that there is no  
542 conflict of interests regarding the publication of this paper. All data used in this paper are available online as  
543 referenced in the 'Methods and Data' section.

#### 544 545 **References**

546 Agarwal, D. A., Humphrey, M., Beekwilder, N. F., Jackson, K. R., Goode, M. M., and van Ingen, C.: A data-centered  
547 collaboration portal to support global carbon-flux analysis, *Concurr. Comp-Pract. E.*, 22, 2323-2334,  
548 <https://doi.org/10.1002/cpe.1600>, 2010.

549 Baldocchi, D., Falge, E., Gu, L., Olson, R., Hollinger, D., Running, S., Anthoni, P., Bernhofer, C., Davis, K., Evans, R.,  
550 Fuentes, J., Goldstein, A., Katul, G., Law, B., Lee, X., Malhi, Y., Meyers, T., Munger, W., Oechel, W., Paw U, K. T.,  
551 Pilegaard, K., Schmid, H. P., Valentini, R., Verma, S., Vesala, T., Wilson, K., and Wofsy, S.: FLUXNET: A New Tool

552 to Study the Temporal and Spatial Variability of Ecosystem-Scale Carbon Dioxide, Water Vapor, and Energy Flux  
553 Densities, B. Am. Meteorol. Soc., 82, 2415-2434, [https://doi.org/10.1175/1520-0477\(2001\)082<2415:FANTTS>2.3.CO;2](https://doi.org/10.1175/1520-0477(2001)082<2415:FANTTS>2.3.CO;2), 2001.

554 Budyko, M. I.: Climate and Life. Academic Press, London, 1974.

555 Choudhury, B. J.: Evaluation of an empirical equation for annual evaporation using field observations and results  
556 from a biophysical model, J. Hydrol., 216, 99-110, [https://doi.org/10.1016/S0022-1694\(98\)00293-5](https://doi.org/10.1016/S0022-1694(98)00293-5), 1999.

557 Dee, D. P., Uppala, S. M., Simmons, A. J., Berrisford, P., Poli, P., Kobayashi, S., Andrae, U., Balmaseda, M. A.,  
558 Balsamo, G., Bauer, P., Bechtold, P., Beljaars, A. C. M., van de Berg, L., Bidlot, J., Bormann, N., Delsol, C., Dragani,  
559 R., Fuentes, M., Geer, A. J., Haimberger, L., Healy, S. B., Hersbach, H., Hólm, E. V., Isaksen, I., Kållberg, P., Köhler,  
560 M., Matricardi, M., McNally, A. P., Monge-Sanz, B. M., Morcrette, J. J., Park, B. K., Peubey, C., de Rosnay, P.,  
561 Tavolato, C., Thépaut, J. N., and Vitart, F.: The ERA-Interim reanalysis: configuration and performance of the  
562 data assimilation system, Q. J. R. Meteorol. Soc., 137, 553-597, <https://doi.org/10.1002/qj.828>, 2011.

563 Donohue, R. J., Roderick, M. L., and McVicar, T. R.: Can dynamic vegetation information improve the accuracy of  
564 Budyko's hydrological model?, J. Hydrol., 390, 23-34, <https://doi.org/10.1016/j.jhydrol.2010.06.025>, 2010.

565 Fu, B. P.: On the Calculation of the Evaporation from Land Surface, Sci. Atmos. Sin., 5, 23-31, 1981.

566 [Gudmundsson, L., Greve, P., and Seneviratne, S. I.: The sensitivity of water availability to changes in the aridity  
567 index and other factors—A probabilistic analysis in the Budyko space, Geophys. Res. Lett., 43, 6985-6994,  
568 <https://doi.org/10.1002/2016GL069763>, 2016.](https://doi.org/10.1002/2016GL069763)

569 Harris, I., Jones, P. D., Osborn, T. J., and Lister, D. H.: Updated high-resolution grids of monthly climatic  
570 observations—the CRU TS3.10 Dataset, Int. J. Climatol., 34, 623-642, <https://doi.org/10.1002/joc.3711>, 2014.

571 Huning, L. S., and AghaKouchak, A.: Mountain snowpack response to different levels of warming, Proc. Natl.  
572 Acad. Sci. U. S. A., 115, 10932, <https://doi.org/10.1073/pnas.1805953115>, 2018.

573 Jackson, R. B., Canadell, J., Ehleringer, J. R., Mooney, H. A., Sala, O. E., and Schulze, E. D.: A Global Analysis of  
574 Root Distributions for Terrestrial Biomes, Oecologia, 108, 389-411, <https://doi.org/10.1007/BF00333714>, 1996.

575 Jung, M., Reichstein, M., Ciais, P., Seneviratne, S. I., Sheffield, J., Goulden, M. L., Bonan, G., Cescatti, A., Chen, J.,  
576 de Jeu, R., Dolman, A. J., Eugster, W., Gerten, D., Gianelle, D., Gobron, N., Heinke, J., Kimball, J., Law, B. E.,  
577 Montagnani, L., Mu, Q., Mueller, B., Oleson, K., Papale, D., Richardson, A. D., Rouspard, O., Running, S., Tomelleri,  
578 E., Viovy, N., Weber, U., Williams, C., Wood, E., Zaehle, S., and Zhang, K.: Recent decline in the global land  
579

580 evapotranspiration trend due to limited moisture supply, *Nature*, 467, 951,  
581 <https://doi.org/10.1038/nature09396>, 2010.

582 Koster, R. D., and Suarez, M. J.: A Simple Framework for Examining the Interannual Variability of Land Surface  
583 Moisture Fluxes, *J. Clim.*, 12, 1911-1917, [https://doi.org/10.1175/1520-0442\(1999\)012<1911:ASFFET>2.0.CO;2](https://doi.org/10.1175/1520-0442(1999)012<1911:ASFFET>2.0.CO;2),  
584 1999.

585 McMahon, T. A., Peel, M. C., Pegram, G. G. S., and Smith, I. N.: A Simple Methodology for Estimating Mean and  
586 Variability of Annual Runoff and Reservoir Yield under Present and Future Climates, *J. Hydrometeorol.*, 12, 135-  
587 146, <https://doi.org/10.1175/2010jhm1288.1>, 2011.

588 Milly, P. C. D.: Climate, soil water storage, and the average annual water balance, *Water Resour. Res.*, 30, 2143-  
589 2156, <https://doi.org/10.1029/94WR00586>, 1994a.

590 Milly, P. C. D.: Climate, interseasonal storage of soil water, and the annual water balance, *Adv. Water Resour.*,  
591 17, 19-24, [https://doi.org/10.1016/0309-1708\(94\)90020-5](https://doi.org/10.1016/0309-1708(94)90020-5), 1994b.

592 Milly, P. C. D., and Dunne, K. A.: Macroscale water fluxes 1. Quantifying errors in the estimation of basin mean  
593 precipitation, *Water Resour. Res.*, 38, 23-21-23-14, <https://doi.org/10.1029/2001WR000759>, 2002a.

594 Milly, P. C. D., and Dunne, K. A.: Macroscale water fluxes 2. Water and energy supply control of their interannual  
595 variability, *Water Resour. Res.*, 38, 24-21-24-29, <https://doi.org/10.1029/2001WR000760>, 2002b.

596 Mueller, B., Hirschi, M., Jimenez, C., Ciais, P., Dirmeyer, P. A., Dolman, A. J., Fisher, J. B., Jung, M., Ludwig, F.,  
597 Maignan, F., Miralles, D. G., McCabe, M. F., Reichstein, M., Sheffield, J., Wang, K., Wood, E. F., Zhang, Y., and  
598 Seneviratne, S. I.: Benchmark products for land evapotranspiration: LandFlux-EVAL multi-data set synthesis,  
599 *Hydrol. Earth. Syst. Sci.*, 17, 3707-3720, <https://doi.org/10.5194/hess-17-3707-2013>, 2013.

600 Norby, R. J., Ledford, J., Reilly, C. D., Miller, N. E., and O'Neill, E. G.: Fine-root production dominates response of  
601 a deciduous forest to atmospheric CO<sub>2</sub> enrichment, *Proc. Natl. Acad. Sci. U. S. A.*, 101, 9689-9693,  
602 <https://doi.org/10.1073/pnas.0403491101>, 2004.

603 [Orth, R., and Destouni, G.: Drought reduces blue-water fluxes more strongly than green-water fluxes in Europe,](https://doi.org/10.1038/s41467-018-06013-7)  
604 [Nat. Commun.](https://doi.org/10.1038/s41467-018-06013-7), 9, 3602, <https://doi.org/10.1038/s41467-018-06013-7>, 2018.

605 Rodell, M., Beaudoin, H. K., L'Ecuyer, T. S., Olson, W. S., Famiglietti, J. S., Houser, P. R., Adler, R., Bosilovich, M.  
606 G., Clayson, C. A., Chambers, D., Clark, E., Fetzer, E. J., Gao, X., Gu, G., Hilburn, K., Huffman, G. J., Lettenmaier,  
607 D. P., Liu, W. T., Robertson, F. R., Schlosser, C. A., Sheffield, J., and Wood, E. F.: The Observed State of the Water

608 Cycle in the Early Twenty-First Century, *J. Clim.*, 28, 8289-8318, <https://doi.org/10.1175/JCLI-D-14-00555.1>,  
609 2015.

610 Roderick, M. L., and Farquhar, G. D.: A simple framework for relating variations in runoff to variations in climatic  
611 conditions and catchment properties, *Water Resour. Res.*, 47, <https://doi.org/10.1029/2010WR009826>, 2011.

612 Sankarasubramanian, A., and Vogel, R. M.: Annual hydroclimatology of the United States, *Water Resour. Res.*,  
613 38, 19-11-19-12, <https://doi.org/10.1029/2001WR000619>, 2002.

614 Scanlon, B. R., Zhang, Z., Save, H., Sun, A. Y., Müller Schmied, H., van Beek, L. P. H., Wiese, D. N., Wada, Y., Long,  
615 D., Reedy, R. C., Longuevergne, L., Döll, P., and Bierkens, M. F. P.: Global models underestimate large decadal  
616 declining and rising water storage trends relative to GRACE satellite data, *Proc. Natl. Acad. Sci. U. S. A.*,  
617 <https://doi.org/10.1073/pnas.1704665115>, 2018.

618 Sposito, G.: Understanding the Budyko Equation, *Water*, 9, <https://doi.org/10.3390/w9040236>, 2017.

619 Stackhouse, P. W., Gupta, S. K., Cox, S. J., Mikovitz, J. C., Zhang, T., and Hinkelman, L. M.: The NASA/GEWEX  
620 Surface Radiation Budget Release 3.0: 24.5-Year Dataset. In: *GEWEX News*, No. 1, 2011.

621 Ukkola, A. M., Houghton, N., De Kauwe, M. G., Abramowitz, G., and Pitman, A. J.: FluxnetLSM R package (v1.0):  
622 a community tool for processing FLUXNET data for use in land surface modelling, *Geosci. Model. Dev.*, 10, 3379-  
623 3390, <https://doi.org/10.5194/gmd-10-3379-2017>, 2017.

624 Wang, D., and Alimohammadi, N.: Responses of annual runoff, evaporation, and storage change to climate  
625 variability at the watershed scale, *Water Resour. Res.*, 48, <https://doi.org/10.1029/2011WR011444>, 2012.

626 Wang-Erlandsson, L., Bastiaanssen, W. G. M., Gao, H., Jägermeyr, J., Senay, G. B., van Dijk, A. I. J. M., Guerschman,  
627 J. P., Keys, P. W., Gordon, L. J., and Savenije, H. H. G.: Global root zone storage capacity from satellite-based  
628 evaporation, *Hydrol. Earth Syst. Sci.*, 20, 1459-1481, <https://doi.org/10.5194/hess-2015-533>, 2016.

629 Yang, H., Yang, D., Lei, Z., and Sun, F.: New analytical derivation of the mean annual water-energy balance  
630 equation, *Water Resour. Res.*, 44, <https://doi.org/10.1029/2007WR006135>, 2008.

631 Yang, Y., Donohue, R. J., and McVicar, T. R.: Global estimation of effective plant rooting depth: Implications for  
632 hydrological modeling, *Water Resour. Res.*, 52, 8260-8276, <https://doi.org/10.1002/2016WR019392>, 2016.

633 Zeng, R., and Cai, X.: Assessing the temporal variance of evapotranspiration considering climate and catchment  
634 storage factors, *Adv. Water Resour.*, 79, 51-60, <https://doi.org/10.1016/j.advwatres.2015.02.008>, 2015.

635 Zhang, L., Potter, N., Hickel, K., Zhang, Y., and Shao, Q.: Water balance modeling over variable time scales based  
636 on the Budyko framework – Model development and testing, *J. Hydrol.*, 360, 117-131,  
637 <https://doi.org/10.1016/j.jhydrol.2008.07.021>, 2008.

638 Zhang, Y., Pan, M., Sheffield, J., Siemann, A. L., Fisher, C. K., Liang, M. L., Beck, H. E., Wanders, N., MacCracken,  
639 R. F., Houser, P. R., Zhou, T., Lettenmaier, D. P., Ma, Y., Pinker, R. T., Bytheway, J., Kummerow, C. D., and Wood,  
640 E. F.: A Climate Data Record (CDR) for the global terrestrial water budget: 1984-2010, *Hydrol. Earth Syst. Sci.*, 22,  
641 241-263, <https://doi.org/10.5194/hess-22-241-2018>, 2018.

642

643

644 **List of Figures:**

645 ~~Figure 1. Spatial mask used in this study.~~

646 Figure 12. Mean annual (1984-2010) (a)  $P$ , (b)  $E$  and (c)  $Q$ .

647 Figure 23. Relationship of mean annual (a) evapotranspiration ( $\bar{E}/\bar{P}$ ) and (b) runoff ( $\bar{Q}/\bar{P}$ ) ratios to the aridity  
648 index ( $\bar{E}_o/\bar{P}$ ) from the CDR and SRB databases.

649 Figure 34. Water cycle variances ( $\sigma_P^2, \sigma_E^2, \sigma_Q^2, \sigma_{\Delta S}^2$ ) and covariances ( $cov(E, Q), cov(E, \Delta S), cov(Q, \Delta S)$ ).

650 ~~Figure 5. Distribution of water cycle variances ( $\sigma_P^2, \sigma_E^2, \sigma_Q^2, \sigma_{\Delta S}^2$ ) and covariances ( $cov(E, Q), cov(E, \Delta S),$   
651  $cov(Q, \Delta S)$ ).~~

652 Figure 46. Relation between inter-annual mean and standard deviation for (a)  $P$ , (b)  $E$  and (c)  $Q$  from the CDR  
653 database.

654 Figure 57. Relationship of inter-annual standard deviation of (a) evapotranspiration ( $\sigma_E/\sigma_P$ ) and (b) runoff ( $\sigma_Q/\sigma_P$ )  
655 ratios to aridity ( $\bar{E}_o/\bar{P}$ ).

656 Figure 68. Relation between water cycle variances-covariances (see Fig-4Fig. 3b-g) as a fraction of the variance  
657 of  $P$  ( $\sigma_P^2$ ) and the aridity index ( $\bar{E}_o/\bar{P}$ ) coloured by density.

658 Figure 79. Relation between water cycle variances-covariances (see Fig-4Fig. 3b-g) as a fraction of the variance  
659 for  $P$  ( $\sigma_P^2$ ) and the aridity index ( $\bar{E}_o/\bar{P}$ ) for grid-cells over different latitude ranges (i.e., 90N-60N, 60N-30N, 30N-  
660 0 and 0-90S). The colours relate to the water storage capacity  $S_{max}$ .

661 Figure 84. Relation between water cycle variances-covariances (see Fig-4Fig. 3b-g) as a fraction of the variance  
662 for  $P$  ( $\sigma_P^2$ ) and the aridity index ( $\bar{E}_o/\bar{P}$ ) for grid-cells over different latitude ranges (i.e., 90N-60N, 60N-30N, 30N-  
663 0 and 0-90S). The colours relate to the mean air temperature ( $\bar{T}_a$ ).

664 Figure 94. Locations of three representative grid-cells used as case study sites.

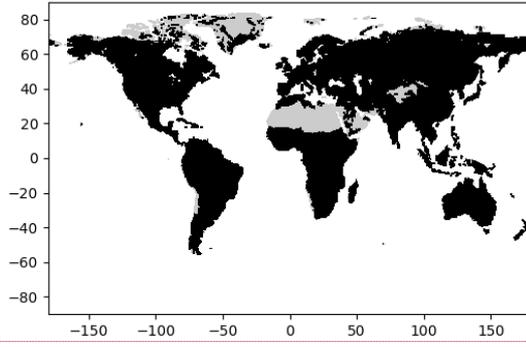
665 Figure 102. Inter-annual time series ( $P, E, Q$  and  $\Delta S$ ) and the associated variance-covariance matrix ( $E, Q$  and  $\Delta S$ )  
666 for case study Sites 1-3.

667 Figure 113. Location of three case study sites in the water cycle variability space.

668 Figure 124. Synthesis of factors controlling variance partitioning.

669

670



671

672

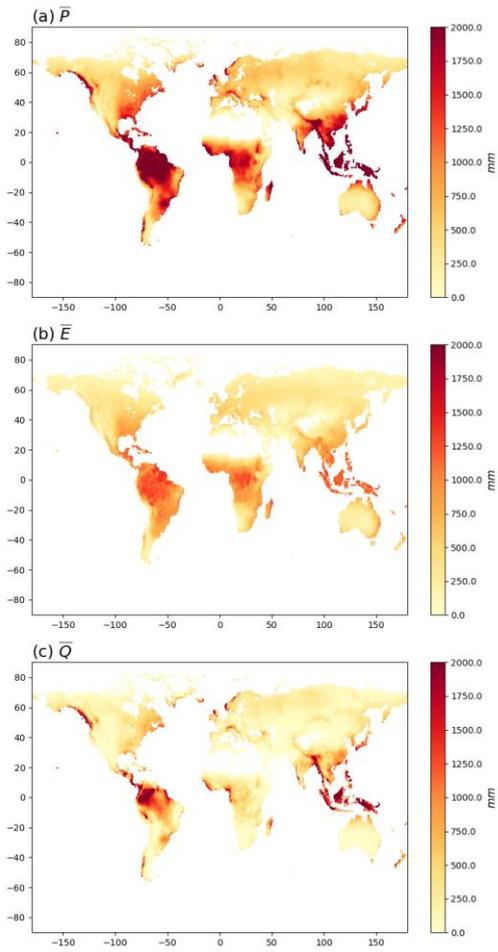
673

674

**Figure 1. Spatial mask used in this study. Grey areas (Himalayan region, Sahara Desert, Greenland) have been masked out of the CDR database.**

Formatted: Font: (Default) Times New Roman, (Asian) MS Mincho, 10 pt, Font color: Text 1

675

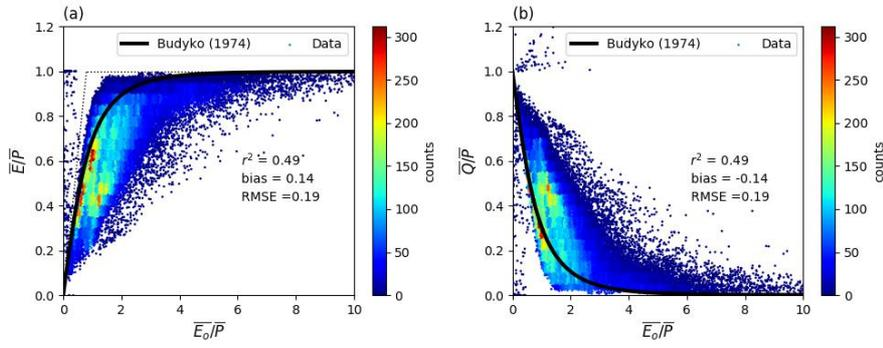


676

677 **Figure 12.** Mean annual (1984-2010) (a)  $P$ , (b)  $E$  and (c)  $Q$ . Note that the mean annual  $\Delta S$  in the CDR database is zero  
678 by construction and is not shown.

679

680

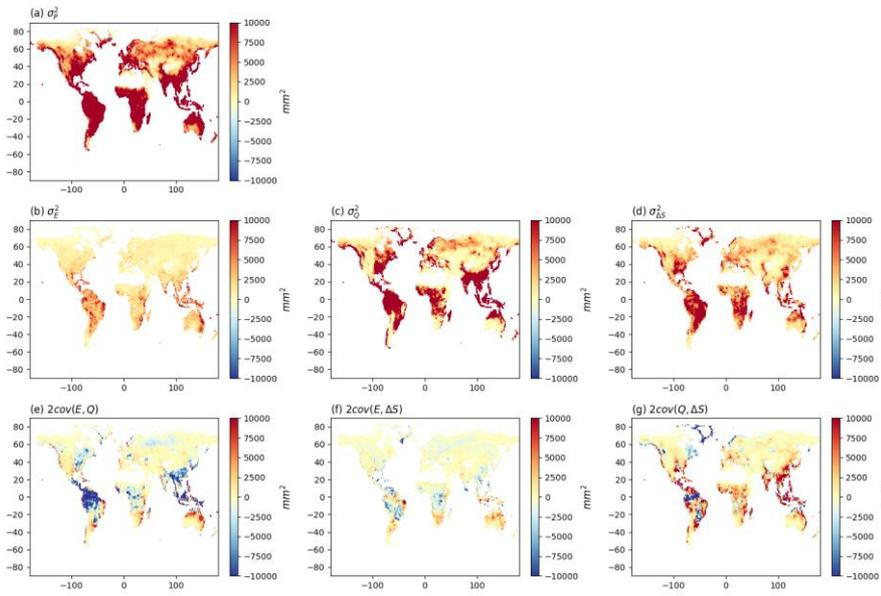


681

682 Figure 23. Relationship of mean annual (a) evapotranspiration ( $\bar{E}/\bar{P}$ ) and (b) runoff ( $\bar{Q}/\bar{P}$ ) ratios to the aridity index  
683 ( $\bar{E}_0/\bar{P}$ ) from the CDR and SRB databases. For comparison, the Budyko (1974) curve is shown on the left panel (Fig.  
684 3Fig. 2a). The curve on the right panel (Fig. 3Fig. 2b) is calculated assuming a steady state ( $\bar{Q}/\bar{P} = 1 - \bar{E}/\bar{P}$ ).

685

686

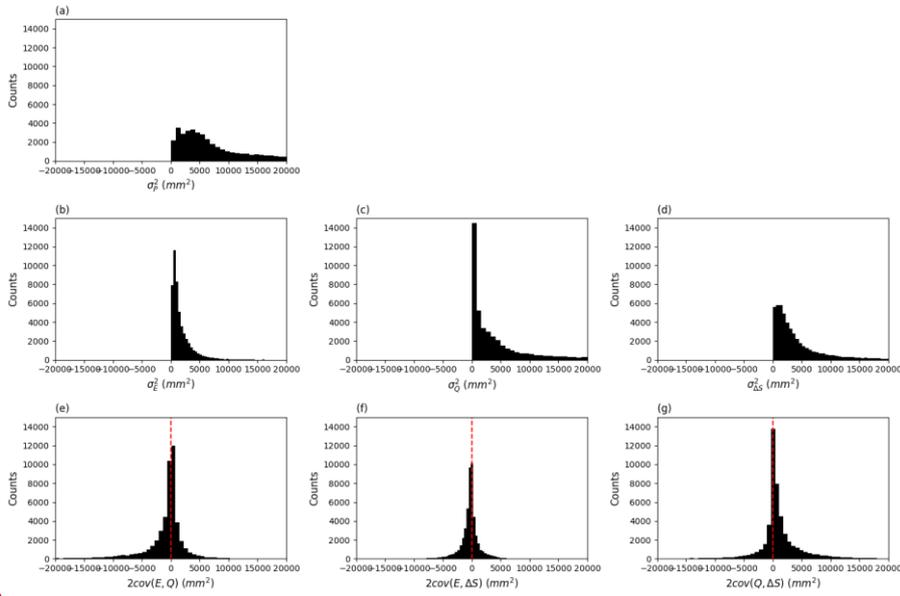


687

688 **Figure 34.** Water cycle variances ( $\sigma_P^2$ ,  $\sigma_E^2$ ,  $\sigma_Q^2$ ,  $\sigma_{\Delta S}^2$ ) and covariances ( $cov(E, Q)$ ,  $cov(E, \Delta S)$ ,  $cov(Q, \Delta S)$ ). Note that we  
689 have multiplied the covariances by two (see Eq. 2).

690

691



692

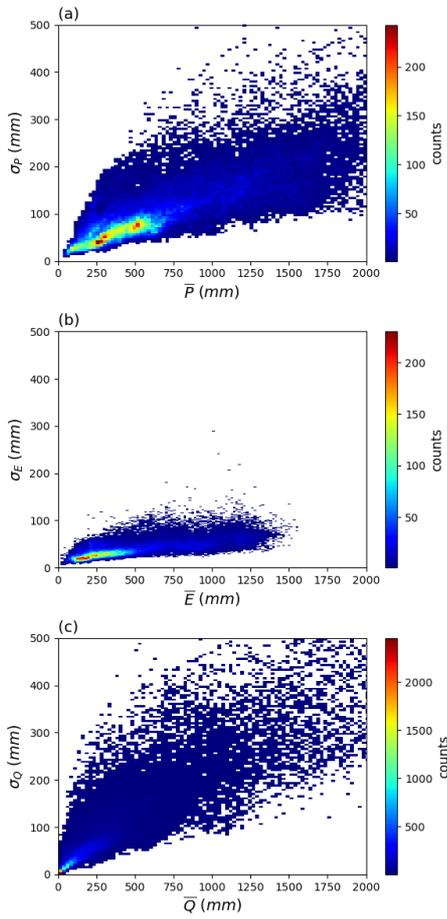
693 **Figure 5.** Distribution of water cycle variances ( $\sigma_p^2, \sigma_e^2, \sigma_{e-p}^2, \sigma_{p-e}^2$ ) and covariances ( $cov(E, Q), cov(E, \Delta S), cov(Q, \Delta S)$ ).

694 **Note that we have multiplied the covariances by two (see Eq. 2).**

695

Formatted: Font: (Default) Times New Roman, 10 pt

696



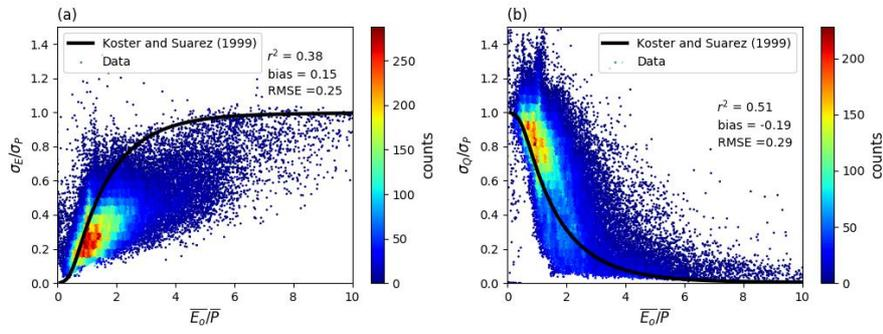
697

698 **Figure 46.** Relation between inter-annual mean and standard deviation for (a)  $P$ , (b)  $E$  and (c)  $Q$  from the CDR

699 database. Note that the mean annual  $\Delta S$  is zero by construction and is not shown.

700

701

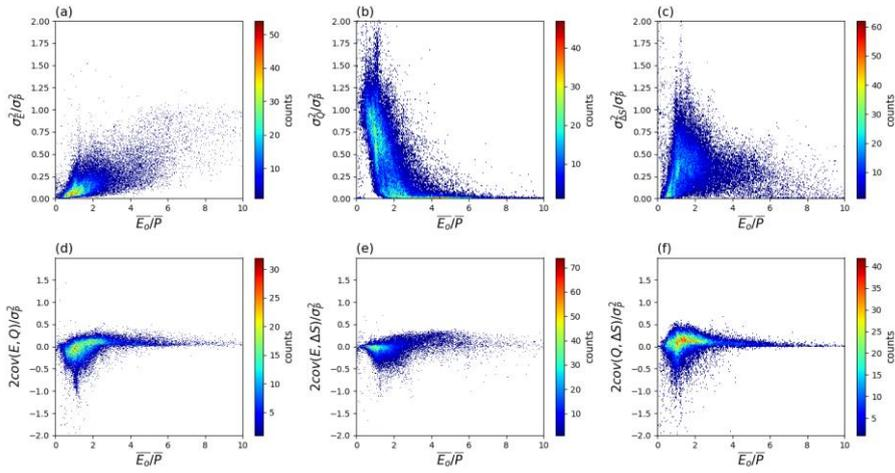


702

703 Figure 57. Relationship of inter-annual standard deviation of (a) evapotranspiration ( $\sigma_E/\sigma_P$ ) and (b) runoff ( $\sigma_Q/\sigma_P$ )  
704 ratios to aridity ( $\overline{E_o/P}$ ). The curves represent the semi-empirical relations from Koster and Suarez (1999).

705

706

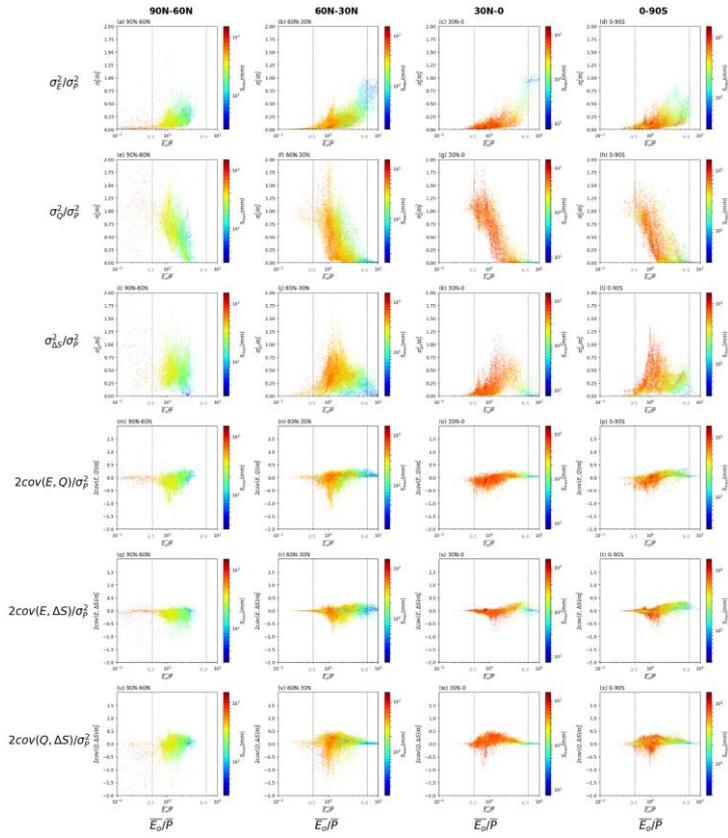


707

708 Figure 68. Relation between water cycle variances-covariances (see Fig-4Fig. 3b-g) as a fraction of the variance of  $P$   
709 ( $\sigma_P^2$ ) and the aridity index ( $\bar{E}_0/\bar{P}$ ) coloured by density. Note that we have multiplied the covariance components by two  
710 (see Eq. 2).

711

712

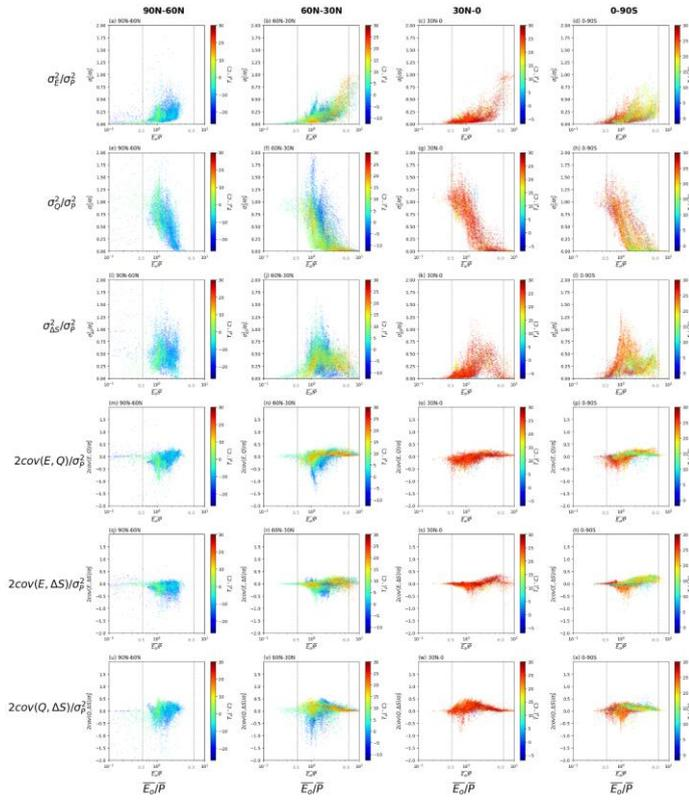


713

714 Figure 79. Relation between water cycle variances-covariances (see Fig. 4 Fig. 3b-g) as a fraction of the variance for  $P$   
 715 ( $\sigma_P^2$ ) and the aridity index ( $\overline{E_0}/\overline{P}$ ) for grid-cells over different latitude ranges (i.e., 90N-60N, 60N-30N, 30N-0 and 0-  
 716 90S). The colours relate to the water storage capacity  $S_{max}$ . Note that we have multiplied the covariances by two (see  
 717 Eq. 2). The vertical grey dashed lines represent thresholds used to separate extremely dry ( $\overline{E_0}/\overline{P} \geq 6.0$ ) and wet  
 718 ( $\overline{E_0}/\overline{P} \leq 0.5$ ) environments. Note the use of a logarithmic x-axis and scale bar for  $S_{max}$ .

719

720

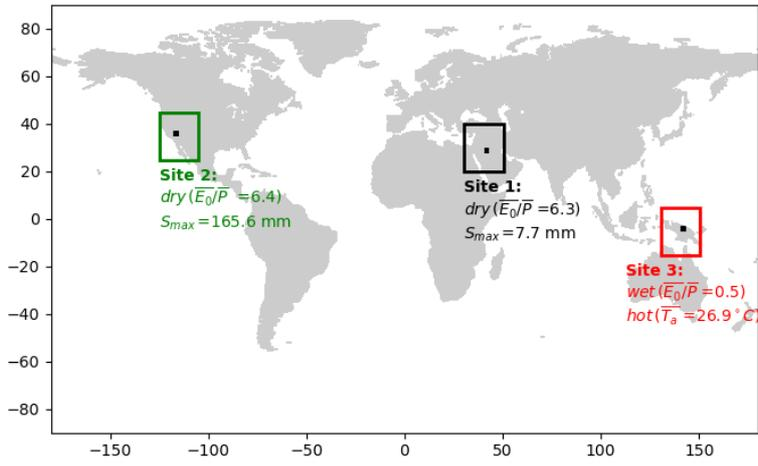


721

722 Figure 810. Relation between water cycle variances-covariances (see Fig-4Fig. 3b-g) as a fraction of the variance for  
 723  $P$  ( $\sigma_P^2$ ) and the aridity index ( $\overline{E_0/P}$ ) for grid-cells over different latitude ranges (i.e., 90N-60N, 60N-30N, 30N-0 and 0-  
 724 90S). The colours relate to the mean air temperature ( $\overline{T_a}$ ). Note that we have multiplied the covariances by two (see  
 725 Eq. 2). The vertical grey dashed lines represent thresholds used to separate extremely dry ( $\overline{E_0/P} \geq 6.0$ ) and wet  
 726 ( $\overline{E_0/P} \leq 0.5$ ) environments.

727

728

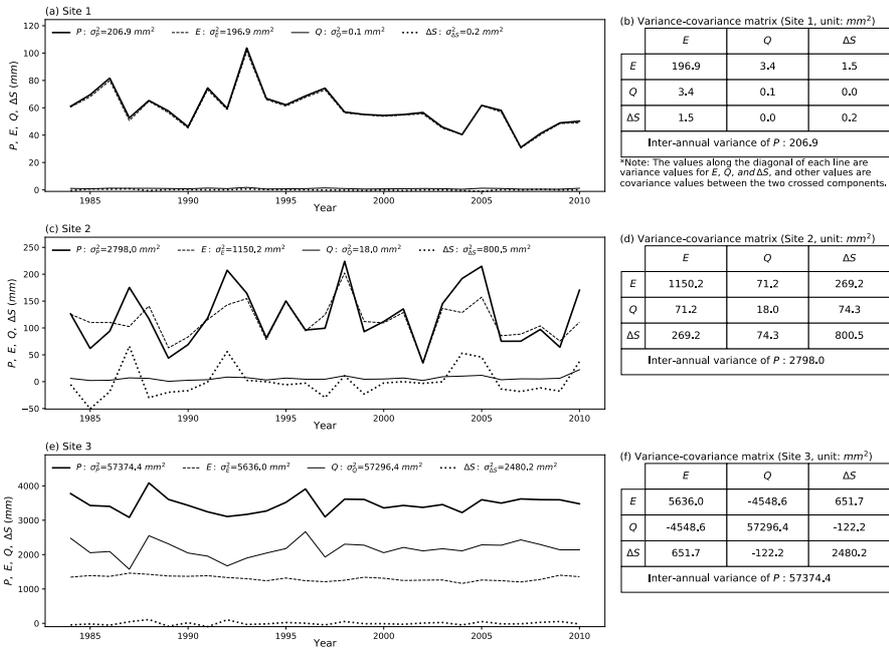


729

730 Figure 911. Locations of three representative grid-cells used as case study sites.

731

732



733

734

735

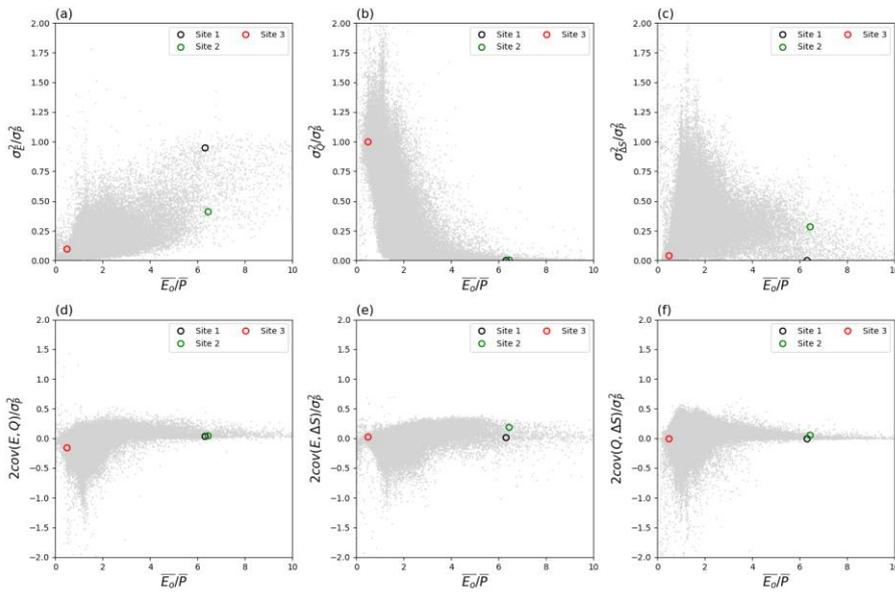
736

737

738

**Figure 102.** Inter-annual time series ( $P$ ,  $E$ ,  $Q$  and  $\Delta S$ ) and the associated variance-covariance matrix ( $E$ ,  $Q$  and  $\Delta S$ ) for case study Sites 1-3. Left column shows time series for (a) Site 1, (c) Site 2 and (e) Site 3, with right column i.e., (b), (d) and (f), the associated variance-covariance matrix for three sites. Note that the covariance values in the tables should be multiplied by two to agree with the variance-covariance balance in Eq. (2).

739

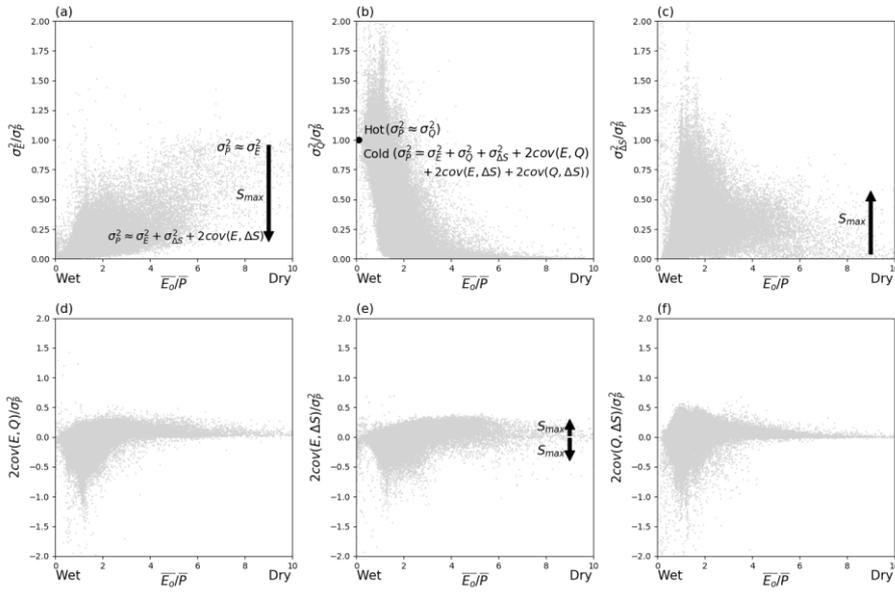


740

741 Figure 113. Location of three case study sites in the water cycle variability space. The grey background dots are from  
742 Fig. 8 Fig. 6.

743

744



745

746 Figure 124. Synthesis of factors controlling variance partitioning. The arrows denote trends with increasing  $S_{max}$ . The  
 747 grey background dots are from Fig. 8 Fig. 6.

748

# Inter-annual variability of the global terrestrial water cycle

Dongqin Yin<sup>1,2</sup>, Michael L. Roderick<sup>1,2,3</sup>

<sup>1</sup>Research School of Earth Sciences, Australian National University, Canberra, ACT, 2601, Australia

<sup>2</sup>Australian Research Council Centre of Excellence for Climate System Science, Canberra, ACT, 2601, Australia

<sup>3</sup>Australian Research Council Centre of Excellence for Climate Extremes, Canberra, ACT, 2601, Australia

## Supplementary Material

This Supplementary Material contains Figures S1-S~~12~~[10](#) and Table S1.

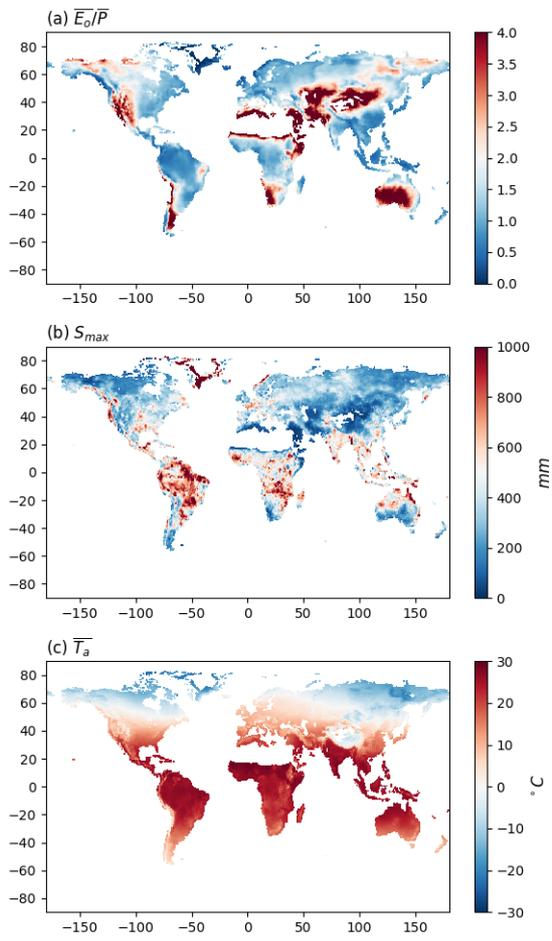
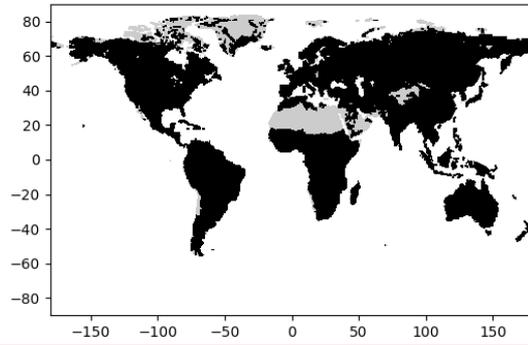


Figure S1. (a) Aridity index ( $\overline{E_0/P}$ ), (b) water storage capacity ( $S_{max}$ ) and (c) mean annual air temperature ( $\overline{T_a}$ ) used in the analysis.



**Figure S2. Spatial mask used in this study. Grey areas (e.g., Himalayan region, Sahara Desert, Greenland) have been masked out of the CDR database.**

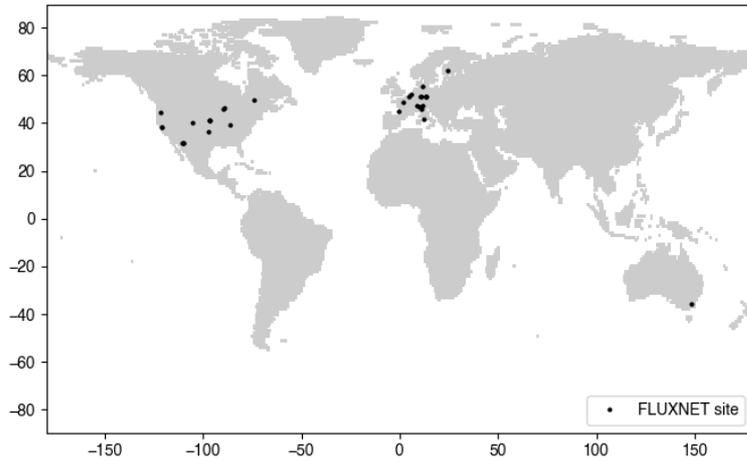


Figure S32. Location of the 32 FLUXNET sites used to evaluate the compared with the Climate Data Record (CDR).





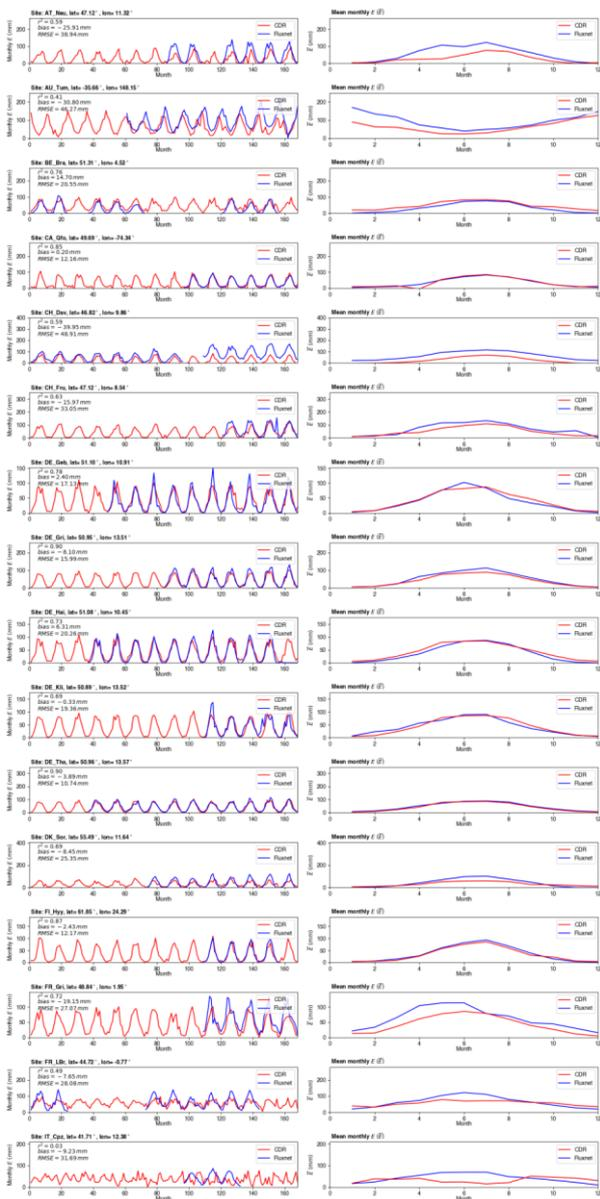


Figure S54. Comparison of monthly evapotranspiration  $E$  time series (left panels) and mean monthly  $E$  (right panels) between FLUXNET site observations and the Climate Data Record (CDR).

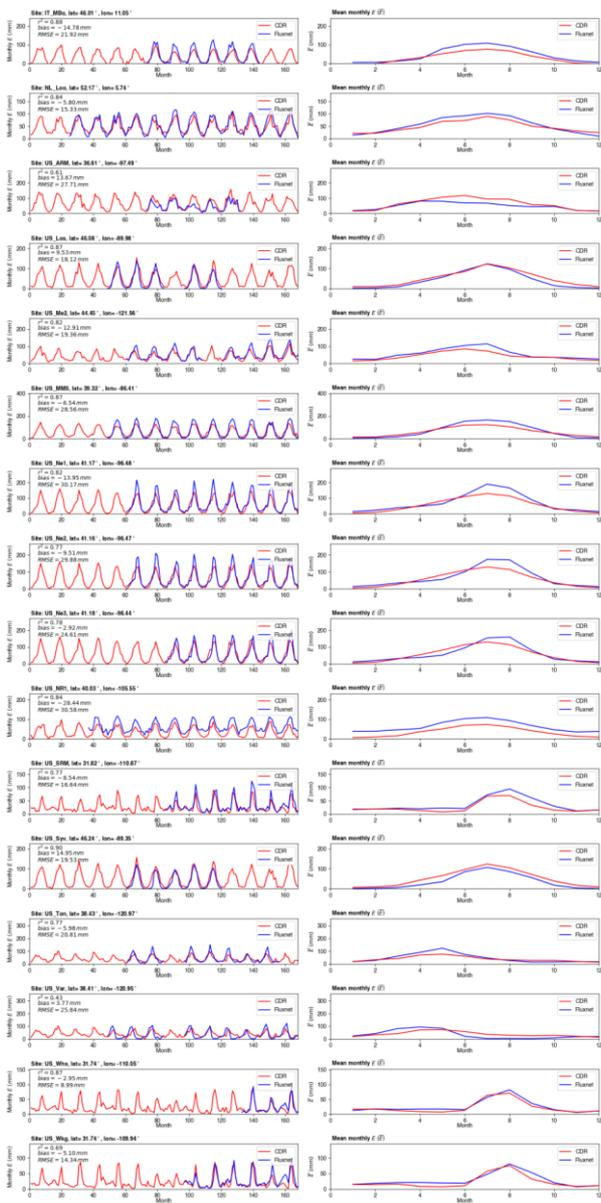
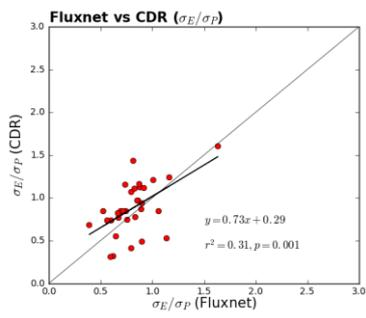
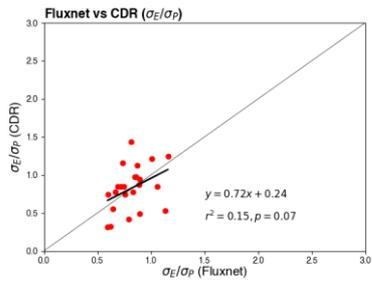


Figure S54 continued.



**Figure S65.** Comparison of ratio of standard deviation of monthly evapotranspiration  $E$  to precipitation  $P$  ( $\sigma_E/\sigma_P$ ) between FLUXNET site observations and the Climate Data Record (CDR).

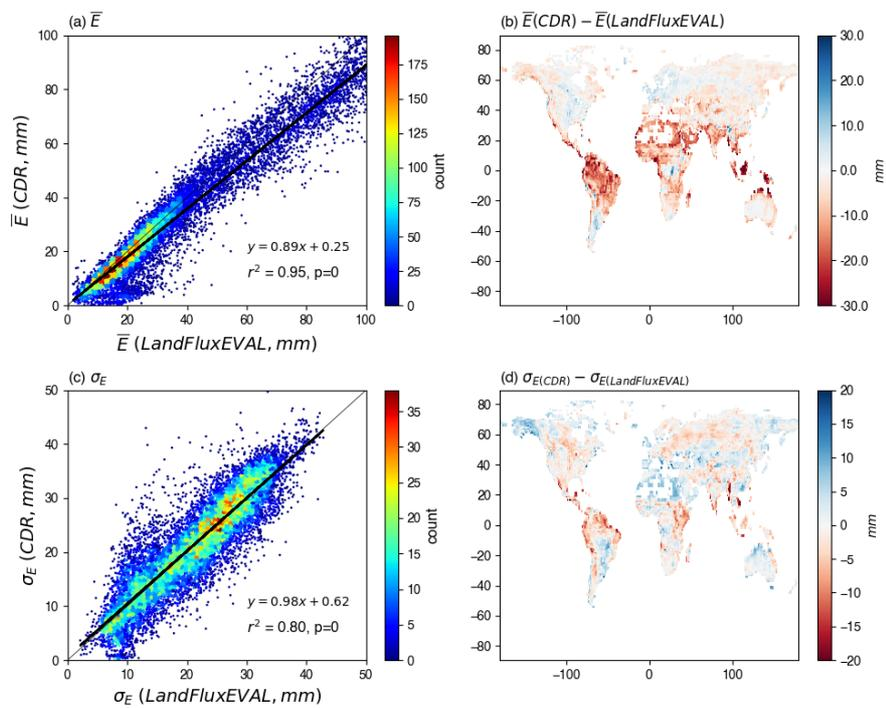


Figure S76. Comparison of monthly evapotranspiration  $E$  between LandFluxEVAL and Climate Data Record (CDR) databases. Top panels (a) (b) show comparison of the mean monthly ( $\bar{E}$ ) while bottom panels (c) (d) show comparison of the standard deviation ( $\sigma_E$ ) of monthly  $E$ .

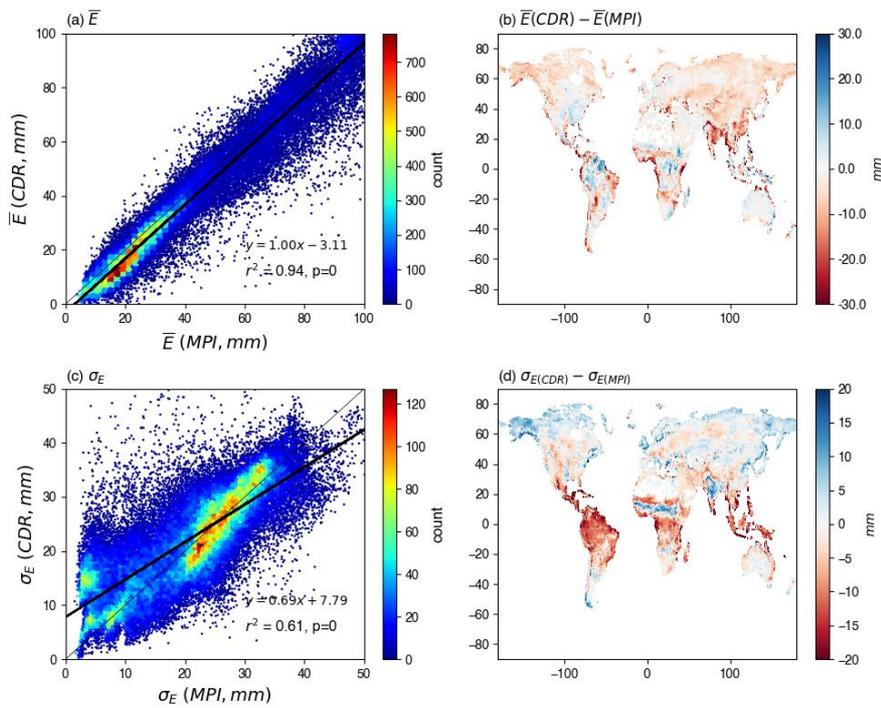
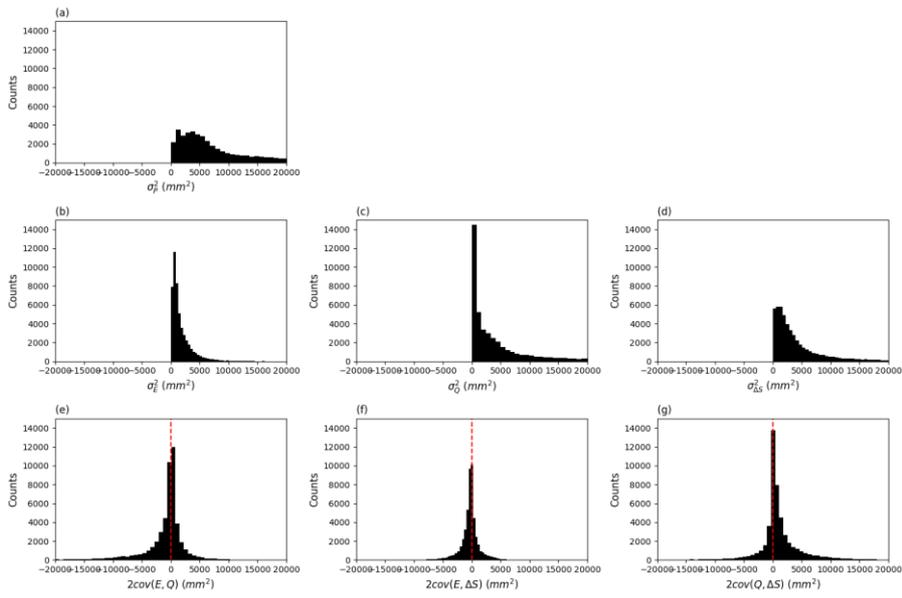
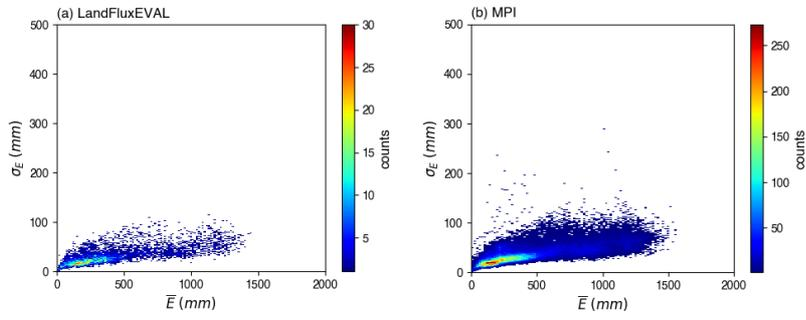


Figure S87. Comparison of monthly evapotranspiration  $E$  between Max Planck Institute (MPI) and Climate Data Record (CDR) databases. Top panels (a) (b) show comparison of the mean monthly ( $\bar{E}$ ) while bottom panels (c) (d) show comparison of the standard deviation ( $\sigma_E$ ) of monthly  $E$ .



**Figure S9.** Distribution for each of the  $\phi$ -water cycle variances ( $\sigma_P^2, \sigma_E^2, \sigma_Q^2, \sigma_{\Delta S}^2$ ) and covariances ( $cov(E, Q), cov(E, \Delta S), cov(Q, \Delta S)$ ) shown in Fig. 3. Note that we have multiplied the covariances by two (see Eq. 2).



**Figure S108.** The same as Fig. 46b in main text but using evapotranspiration  $E$  data from the (a) LandFluxEVAL and (b) MPI databases.

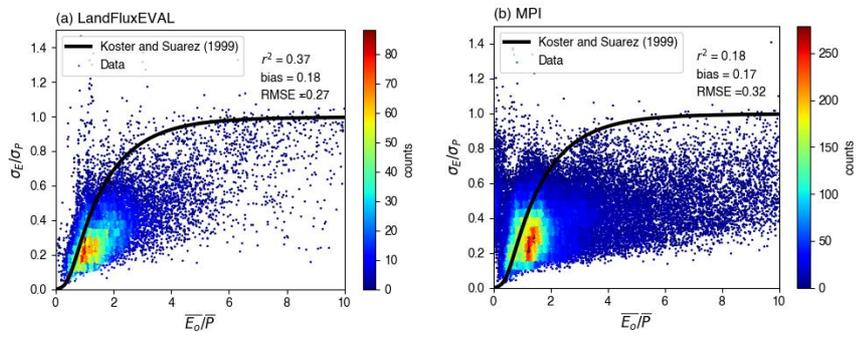
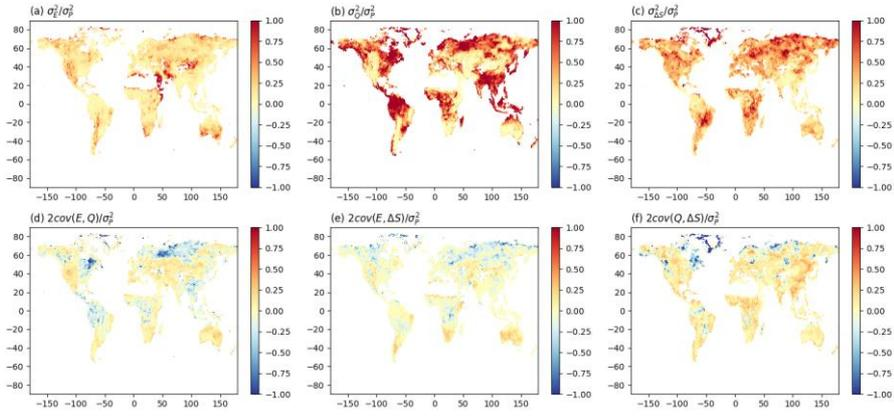


Figure S119. The same as Fig. S7a in main text but using evapotranspiration  $E$  data from the (a) LandFluxEVAL and (b) MPI databases.



**Figure S129.** Inter-annual water cycle variances ( $\sigma_E^2, \sigma_Q^2, \sigma_{\Delta S}^2$ ) and covariances ( $cov(E, Q), cov(E, \Delta S), cov(Q, \Delta S)$ ) expressed as a fraction of the variance of  $P$  ( $\sigma_P^2$ ). Note that we have multiplied the covariances by two (see Eq. 2).

Table S1. Summary of comparisons of monthly precipitation  $P$  and evapotranspiration  $E$  between observations at 32 FLUXNET sites and the CDR database.

Site ID	Site Name	Lat	Lon	Ref	Data period	$r^2$ ( $P$ )	bias ( $P$ , mm)	RMSE ( $P$ , mm)	$r^2$ ( $E$ )	bias ( $E$ , mm)	RMSE ( $E$ , mm)
AT_Neu	Neustift	47.1167	11.3175	Wohlfahrt et al., 2008	2004 - 2005, 2007 - 2010	<b>0.64</b>	53.54	61.53	<b>0.59</b>	-25.91	38.94
AU_Tum	Tumbarumba	-35.6566	148.1517	Leuning et al., 2005	2002 - 2010	<b>0.56</b>	1.08	39.34	<b>0.41</b>	-30.80	46.27
BE_Bra	Brasschaat	51.3076	4.5198	Carrara et al., 2004	1997 - 1998, 2000 -2002, 2007 - 2009	<b>0.64</b>	-3.05	26.66	<b>0.76</b>	14.70	20.55
CA_Qfo	Quebec - Eastern Boreal, Mature Black Spruce	49.6925	-74.3421	Bergeron et al., 2006	2005 - 2010	<b>0.57</b>	4.43	31.77	<b>0.85</b>	0.20	12.16
CH_Dav	Davos	46.8153	9.8559	Zielis et al., 2014	1997 - 2004, 2006 - 2010	<b>0.64</b>	82.53	91.39	<b>0.59</b>	-39.95	48.91
CH_Fru	Früebüel	47.1158	8.5378	Imer et al., 2013	2007 - 2010	<b>0.65</b>	-15.42	55.86	<b>0.63</b>	-15.97	33.05
DE_Geb	Gebesee	51.1001	10.9143	Anthoni et al., 2004	2001 - 2010	<b>0.69</b>	3.78	17.69	<b>0.78</b>	2.40	17.13
DE_Gri	Grillenburg	50.9500	13.5126	Prescher et al., 2010	2004 - 2010	<b>0.70</b>	-26.32	37.67	<b>0.90</b>	-8.10	15.99
DE_Hai	Hainich	51.0792	10.4530	Knohl et al., 2003	2000 - 2012	<b>0.70</b>	-10.35	23.17	<b>0.73</b>	6.31	20.26
DE_Kli	Klingenberg	50.8931	13.5224	Prescher et al., 2010	2006 - 2010	<b>0.68</b>	-13.61	28.05	<b>0.69</b>	-0.33	19.36
DE_Tha	Tharandt	50.9624	13.5652	Grünwald and Bernhofer, 2007	2000 - 2010	<b>0.66</b>	-18.71	32.35	<b>0.90</b>	-3.89	10.74
DK_Sor	Soroe	55.4859	11.6446	Pilegaard et al., 2011	2003 - 2010	<b>0.45</b>	-11.07	39.31	<b>0.69</b>	-8.45	25.35
FI_Hyy	Hyytiala	61.8474	24.2948	Suni et al., 2003	2006 - 2009	<b>0.78</b>	-7.07	20.43	<b>0.87</b>	-2.43	12.17
FR_Gri	Grignon	48.8442	1.9519	Loubet et al., 2011	2006 - 2010	<b>0.69</b>	-0.81	12.35	<b>0.72</b>	-19.15	27.07
FR_LBr	Le Bray	44.7171	-0.7693	Berbigier et al., 2001	1997 -1998, 2003 - 2008	<b>0.56</b>	-9.19	39.93	<b>0.49</b>	-7.65	28.08
IT_Cpz	Castelporziano	41.7053	12.3761	Garbulsy et al., 2008	2005 - 2007	<b>0.76</b>	-15.90	40.42	0.03	-9.23	31.69

<b>IT_MBo</b>	Monte Bondone	46.0147	11.0458	Marcolla et al., 2011	2003 - 2008	<b>0.36</b>	12.43	48.14	<b>0.88</b>	-14.78	21.92
<b>NL_Loo</b>	Loobos	52.1666	5.7436	Moors 2012	1999 - 2010	<b>0.56</b>	-2.16	24.78	<b>0.84</b>	-5.80	15.33
<b>US_ARM</b>	ARM Southern Great Plains site-Lamont	36.6058	-97.4888	Baldocchi and Sturtevant 2015	2003 - 2007	<b>0.71</b>	13.53	31.78	<b>0.61</b>	13.67	27.71
<b>US_Los</b>	Lost Creek	46.0827	-89.9792	Baker et al., 2003	2001 - 2003, 2005 - 2006	<b>0.52</b>	7.76	32.82	<b>0.87</b>	9.53	18.12
<b>US_Me2</b>	Metolius mature ponderosa pine	44.4523	-121.5574	Law (2002-2014)	2002 - 2005, 2007 - 2010	<b>0.54</b>	45.31	56.84	<b>0.82</b>	-12.91	19.36
<b>US_MMS</b>	Morgan Monroe State Forest	39.3232	-86.4131	Novick and Phillips (1999-2014)	2001 - 2010	<b>0.72</b>	6.60	31.44	<b>0.87</b>	-6.54	28.56
<b>US_Ne1</b>	Mead - irrigated continuous maize site	41.1651	-96.4766	Suyker (2001-2013a)	2002 - 2010	<b>0.45</b>	-6.64	51.86	<b>0.82</b>	-13.95	30.17
<b>US_Ne2</b>	Mead - irrigated maize-soybean rotation site	41.1649	-96.4701	Suyker (2001-2013b)	2002 - 2010	<b>0.56</b>	-8.77	46.45	<b>0.77</b>	-9.51	29.88
<b>US_Ne3</b>	Mead - rainfed maize-soybean rotation site	41.1797	-96.4397	Suyker (2001-2013c)	2004 - 2010	<b>0.88</b>	2.28	21.43	<b>0.78</b>	-2.92	24.61
<b>US_NR1</b>	Niwot Ridge Forest (LTER NWT1)	40.0329	-105.5464	Blanken (1998-2014)	2000 - 2010	<b>0.51</b>	-16.06	29.57	<b>0.84</b>	-28.44	30.58
<b>US_SRM</b>	Santa Rita Mesquite	31.8214	-110.8661	Barron-Gafford et al., 2011	2004 - 2010	<b>0.81</b>	1.34	15.40	<b>0.77</b>	-8.54	16.64
<b>US_Syv</b>	Sylvania Wilderness Area	46.2420	-89.3477	Desai et al., 2008	2002 - 2006	<b>0.33</b>	13.17	40.68	<b>0.90</b>	14.95	19.53
<b>US_Ton</b>	Tonzi Ranch	38.4316	-120.9660	Baldocchi et al., 2010	2002 - 2003, 2005 - 2009	<b>0.89</b>	14.68	27.44	<b>0.77</b>	-5.98	20.81

<b>US_Var</b>	Vaira Ranch- Ione	38.4133	-120.9507	Baldocchi et al., 2004	2001 - 2003, 2005 - 2010	<b>0.86</b>	16.91	30.92	<b>0.43</b>	3.77	25.84
<b>US_Whs</b>	Walnut Gulch Lucky Hills Shrub	31.7438	-110.0522	Biederman et al., 2016	2008 - 2010	<b>0.65</b>	1.89	21.26	<b>0.87</b>	-2.95	8.99
<b>US_Wkg</b>	Walnut Gulch Kendall Grasslands	31.7365	-109.9419	Biederman et al., 2016	2005 - 2010	<b>0.78</b>	1.59	15.66	<b>0.69</b>	-5.10	14.34

\* Significant  $r^2$  values (linear regression  $p < 0.05$ ) are shown in bold.

## References

- Anthoni, P. M., and Coauthors, 2004: Forest and agricultural land-use-dependent CO<sub>2</sub> exchange in Thuringia, Germany. *Global Change Biology*, **10**, 2005-2019.
- B., L., and Coauthors, 2011: Carbon, nitrogen and Greenhouse gases budgets over a four years crop rotation in northern France. *Plant and Soil*, **343**, 109-137.
- Baker, I., and Coauthors, 2003: Simulated And Observed Fluxes Of Sensible And Latent Heat And CO<sub>2</sub> At The WLEF-TV Tower Using SiB2.5. *Global Change Biology*, **9**, 1262-1277.
- Baldocchi, D., and C. Sturtevant, 2015: Does day and night sampling reduce spurious correlation between canopy photosynthesis and ecosystem respiration? . *Agricultural and Forest Meteorology*, **207**, 117-126.
- Baldocchi, D. D., L. Xu, and N. Kiang, 2004: How plant functional-type, weather, seasonal drought, and soil physical properties alter water and energy fluxes of an oak-grass savanna and an annual grassland. *Agricultural and Forest Meteorology*, **123**, 13-39.
- Baldocchi, D. D., and Coauthors, 2010: On the differential advantages of evergreenness and deciduousness in mediterranean oak woodlands: a flux perspective. *Ecological Applications*, **20**, 1583-1597.
- Barron-Gafford, G. A., R. L. Scott, G. D. Jenerette, and T. E. Huxman, 2011: The relative controls of temperature, soil moisture, and plant functional group on soil CO<sub>2</sub> efflux at diel, seasonal, and annual scales. *Journal of Geophysical Research: Biogeosciences*, **116**.
- Berbigier, P., J. M. Bonnefond, and P. Mellmann, 2001: CO<sub>2</sub> and water vapour fluxes for 2 years above Euroflux forest site. *Agricultural and Forest Meteorology*, **108**, 183-197.
- Bergeron, O., H. A. Margolis, T. A. Black, C. Coursolle, A. L. Dunn, A. G. Barr, and S. C. Wofsy, 2006: Comparison of carbon dioxide fluxes over three boreal black spruce forests in Canada. *Global Change Biology*, **13**, 89-107.
- Biederman, J. A., and Coauthors, 2016: Terrestrial carbon balance in a drier world: the effects of water availability in southwestern North America. *Global Change Biology*, **22**, 1867-1879.
- Blanken, P., 1998-2014: FLUXNET2015 US-NR1 Niwot Ridge Forest (LTER NWT1).
- Carrara, A., I. A. Janssens, J. Curiel Yuste, and R. Ceulemans, 2004: Seasonal changes in photosynthesis, respiration and NEE of a mixed temperate forest. *Agricultural and Forest Meteorology*, **126**, 15-31.
- Desai, A. R., and Coauthors, 2008: Influence of vegetation and seasonal forcing on carbon dioxide fluxes across the Upper Midwest, USA: Implications for regional scaling. *Agricultural and Forest Meteorology*, **148**, 288-308.
- Garbulsky, M. F., J. Penuelas, D. Papale, and I. Filella, 2008: Remote estimation of carbon dioxide uptake by a Mediterranean forest. *Global Change Biology*, **14**, 2860-2867.
- Grünwald, T., and C. Bernhofer, 2007: A decade of carbon, water and energy flux measurements of an old spruce forest at the Anchor Station Tharandt. *Tellus B Chem. Phys. Meteorol.*, **59**, 387-396.
- Imer, D., L. Merbold, W. Eugster, and N. Buchmann, 2013: Temporal and spatial variations of soil CO<sub>2</sub>, CH<sub>4</sub> and N<sub>2</sub>O fluxes at three differently managed grasslands. *Biogeosciences*, **10**, 5931-5945.
- Knohl, A., E. D. Schulze, O. Kolle, and N. Buchmann, 2003: Large carbon uptake by an unmanaged 250-year-old deciduous forest in Central Germany. *Agricultural and Forest Meteorology*, **118**, 151-167.
- Law, B., 2002-2014: FLUXNET2015 US-Me2 Metolius mature ponderosa pine.
- Leuning, R., H. A. Cleugh, S. J. Zegelin, and D. Hughes, 2005: Carbon and water fluxes over a temperate Eucalyptus forest and a tropical wet/dry savanna in Australia: measurements and comparison with MODIS remote sensing estimates. *Agricultural and Forest Meteorology*, **129**, 151-173.
- Marcolla, B., and Coauthors, 2011: Climatic controls and ecosystem responses drive the inter-annual variability of the net ecosystem exchange of an alpine meadow. *Agricultural and Forest Meteorology*, **151**, 1233-1243.
- Moors, E. J., 2012: Water Use of Forests in The Netherlands. PhD-thesis, Vrije Universiteit Amsterdam.
- Novick, K., and R. Phillips, 1999-2014: FLUXNET2015 US-MMS Morgan Monroe State Forest.
- Pilegaard, K., A. Ibrom, M. S. Courtney, P. Hummelshøj, and N. O. Jensen, 2011: Increasing net CO<sub>2</sub> uptake by a Danish beech forest during the period from 1996 to 2009. *Agricultural and Forest Meteorology*, **151**, 934-946.
- Prescher, A. K., T. Grunwald, and C. Bernhofer, 2010: Land use regulates carbon budgets in eastern Germany: From NEE to NBP. *Agricultural and Forest Meteorology*, **150**, 1016-1025.
- Suni, T., and Coauthors, 2003: Long-term measurements of surface fluxes above a Scots pine forest in Hyytiälä, southern Finland, 1996-2001. *Boreal Environment Research*, **8**, 287-301.
- Suyker, A., 2001-2013a: FLUXNET2015 US-Ne3 Mead - rainfed maize-soybean rotation site.
- Suyker, A., 2001-2013b: FLUXNET2015 US-Ne2 Mead - irrigated maize-soybean rotation site.
- Suyker, A., 2001-2013c: FLUXNET2015 US-Ne1 Mead - irrigated continuous maize site.

Wohlfahrt, G., A. Hammerle, A. Haslwanter, M. Bahn, U. Tappeiner, and A. Cernusca, 2008: Seasonal and inter-annual variability of the net ecosystem CO<sub>2</sub> exchange of a temperate mountain grassland: effects of climate and management. *Journal of Geophysical Research: Atmospheres* **113**, D08110.

Zielis, S., S. Etzold, R. Zweifel, W. Eugster, M. Haeni, and N. Buchmann, 2014: NEP of a Swiss subalpine forest is significantly driven not only by current but also by previous year's weather. *Biogeosciences*, **11**, 1627-1635.